

A controllable two-qubit swapping gate using superconducting circuits

S. E. Rasmussen,^{1,*} K. S. Christensen,¹ and N. T. Zinner^{1,2,†}

¹*Department of Physics and Astronomy, Aarhus University, DK-8000 Aarhus C, Denmark*

²*Aarhus Institute of Advanced Studies, Aarhus University, DK-8000 Aarhus C, Denmark*

(Dated: December 15, 2024)

In this paper we investigate a linear chain of qubits and determine that it can be configured into a conditional two-qubit swapping gate, where the first and last qubit of the chain are the swapped qubits, and the remaining middle ancilla qubits are controlling the state of the gate. The swapping gate introduces different phases on the final states depending on the initial states. In particular we focus on a chain of four qubits and show the swapping gate it implements. We simulate the chain with decoherence noise and leakage to higher excited states, and find an average fidelity of around 0.99. We propose a superconducting circuit which implements this chain of qubits and present a circuit design of the circuit. We also discuss how to operate the superconducting circuit such that the state of the gate can be controlled. Lastly, we discuss how the circuit can be straightforwardly altered and may be used to simulate Hamiltonians with non-trivial topological properties.

I. INTRODUCTION

A universal set of quantum gates can consist entirely of two-qubit gates [1]. If a quantum information processor is to be created it is therefore desirable to have a number of two-qubit gates which can be implemented without too much difficulty. One of the most promising candidates for the base of such a processor is superconducting qubits, where single-qubit gate operations are performed with gate fidelities well above 0.99 [2–8], which is the lower bound for performing fault-tolerant quantum computing, using error correction surface codes [9–12]. However, the fidelity of two-qubit gate are just entering the 0.99 fidelity regime. Fidelities up to 0.994 have been reported in 2014 in a controlled phase gate [8, 13, 14], and in 2016 IBM achieved a fidelity of 0.991 in the cross-resonance gate [15]. Other notable two-qubit gates that have performed with a fidelity of above 0.9 are: The *iSWAP* and \sqrt{iSWAP} gates [7, 16–18], the *bSWAP* gate [19], the resonator induced phase gate [20].

In this paper we investigate what kind of quantum mechanical two-qubit gates a linear chain of qubits implements. We further propose a way of implementing such a chain using superconducting qubits. We show that such a chain, with an average fidelity around 0.99, swaps the end qubits which receive a phase depending on the configuration of the linear chain. The swapping operation is controlled on the middle qubits, acting as ancilla qubits. All in all this implements a conditional two-qubit swapping gate.

This paper is organized as follows: In Section II A we introduce the Hamiltonian of the system, and the requirements to it. This is followed by Section II B where we present the swapping gate which the Hamiltonian implements, and perform a numerical investigation of the average fidelity of the gate when varying the parame-

ters of the system. Then, in Section III A, we present a superconducting circuit which implements the desired Hamiltonian in the case of four qubits. We also present a chip design of the circuit. We discuss the effect of leakage and decoherence noise in a realistic implemented system via a numerical simulation in Section III B. In Section IV we discuss how to mend the superconducting circuit into simulating other quantum systems, and thus showing the utility of the circuit. Finally in Section V we summarize and conclude the paper.

II. THE SYSTEM

We claim that using a linear Heisenberg model we can implement a two qubit swapping gate. We start by presenting the Hamiltonian of the system, and then explains how it yields the gate.

A. The Hamiltonian

The Heisenberg model has many interesting applications on its own, from the study of quantum phase transitions [21, 22] and magnetism [23] to exploring topological states such as spin liquid states [24]. It is also closely related to the Hubbard model. Here we consider a linear Heisenberg spin chain consisting of N spins (or qubits). In the Schrödinger picture the linear Heisenberg spin model takes the form

$$H = -\frac{1}{2} \sum_{j=1}^N \Omega_j \sigma_j^z + \sum_{j=1}^{N-1} [J_j^x (\sigma_j^x \sigma_{j+1}^x + \sigma_j^y \sigma_{j+1}^y) + J_j^z (\sigma_j^z \sigma_{j+1}^z)], \quad (1)$$

where $\sigma_j^{x,y,z}$ are the Pauli spin matrices, Ω_j denotes the frequency of qubit j , and the $J_j^{x,z}$'s denotes the coupling

* stig.elkjaer.rasmussen@post.au.dk

† zinner@phys.au.dk

between the j 'th and $(j+1)$ 'th qubit. This means that we consider only nearest neighbor XXZ interactions. Note that we use $\hbar = 2e = 1$ throughout this paper.

We now follow Ref. [25] and assume a spatially symmetric spin chain, meaning that $\Omega_j = \Omega_{N+1-j}$ and $J_j^{x,z} = J_{N-j}^{x,z}$. In order to study the role of the interactions we transform into the interaction picture choosing the non-interacting Hamiltonian as

$$H_0 = -\frac{1}{2}\Omega_1 \sum_{j=1}^N \sigma_j^z, \quad (2)$$

which yields the interaction Hamiltonian

$$H_I = -\frac{1}{2} \sum_{j=2}^{N-1} \Delta_j \sigma_j^z + \sum_{j=1}^{N-1} [J_j^x (\sigma_j^x \sigma_{j+1}^x + \sigma_j^y \sigma_{j+1}^y) + J_j^z \sigma_j^z \sigma_{j+1}^z], \quad (3)$$

where the detuning is $\Delta_j = \Omega_j - \Omega_1$ and we have used the rotating wave approximation to neglect interaction terms which obtain a time-dependent phase of $e^{\pm 2i\Omega_1 t}$. This is justified under the assumption that $\Omega_1 \gg J_j$, which is valid for the rest of the paper.

Although the result of Ref. [25] is valid for any $N \geq 4$ we will now focus on the case of $N = 4$. This is partly due to the fact that it simplifies the arguments while the ideas remain intact, and partly due to the fact that a physical implementation, as discussed in Section III, is more easily done with fewer qubits. See Appendix 2 for a discussion on the case of five qubits. With only four qubits we are left with just one detuning, why we drop the subscript, $\Delta \equiv \Delta_2$, and four interaction terms, $J_{1,2}^{x,z}$. The last requirements for the gate relates these parameters; the first is $\Delta = \Delta_{\pm} \equiv 2(J_2^z \pm J_2^x)$ in accordance with Ref. [25], while the second requirement is $J_1 \equiv J_1^x = J_1^z$. For a derivation of these requirements see Appendix 1. A schematic model of the system is seen in Fig. 2(a).

B. The two-qubit swapping gate

We claim that the above Hamiltonian, consisting of four qubits, implements a two-qubit swapping gate, where the first and the last qubits are the swapped qubits, while the middle ancilla qubits control the state of the gate. We thus have a multi-qubit controlled gate, where the combined state of the control qubits determine the state of the gate, effectively working as a single control qubit [26–28]. The control qubits then constitutes a switch which can either be in an “open”-state, which, in the case of four qubit, i.e. two control qubits, is $|0\rangle_C \equiv |00\rangle_C$, or and “closed”-state, which, in this case is the Bell states $|1^{\pm}\rangle_C = (|10\rangle_C \pm |01\rangle_C)/\sqrt{2}$, depending on the choice of Δ_{\pm} . Note that the subscript C denotes the $(N-2)$ -qubit state of the control qubits, while we use T for the target,

i.e. first and last, qubits. In the computational basis of the target qubits, $\{|00\rangle_T, |01\rangle_T, |10\rangle_T, |11\rangle_T\}$, the open gate can be expressed as

$$U_{\text{open}} = \begin{pmatrix} 1 & 0 & 0 & 0 \\ 0 & 0 & \mp 1 & 0 \\ 0 & \mp 1 & 0 & 0 \\ 0 & 0 & 0 & i \end{pmatrix}, \quad (4)$$

where the choice of Δ_{\pm} dictates the phase on the swap. The closed state of the gate is simply the identity $U_{\text{closed}} = \mathbb{1}_4$. The open gate will entangle the input and output qubits. This can be quantified using the entanglement power [29] which in our case is 1/9.

In order to quantify the effectiveness of the gate, we use numerical simulations with realistic gate parameters for state-of-the-art superconducting circuits. In Fig. 4 we show simulations of the gate in a circuit with specific superconducting circuit parameters. We include decoherence noise occurring in superconducting circuits by considering the Lindblad master equation

$$\dot{\rho} = -i[H, \rho] + \gamma \sum_j \left[A_l \rho A_l - \frac{1}{2} (\rho A_l^2 + A_l^2 \rho) \right], \quad (5)$$

where ρ is the density matrix, H is the Hamiltonian in Eq. (3), and the sum is taken over the eight collapse operators A_l : σ_j^z inducing dephasing, and σ_j^- inducing photon loss, with j running over all qubits. We take the decoherence rate, γ , to be identical on all qubits with a state-of-the-art rate of $\gamma = 0.01$ MHz giving the qubits a life-time of 100 μ s [30].

In order to measure the quality of the gate we consider the average fidelity [31]

$$\bar{F}(t) = \frac{1}{5} + \frac{1}{80} \sum_{j=1}^{16} \text{Tr} \left(U_{\text{target}} U_j^{\dagger} U_{\text{target}}^{\dagger} \mathcal{E}_t(U_j) \right), \quad (6)$$

which evaluates how well a quantum map, \mathcal{E}_t , approximates the target gate, U_{target} , over a uniform distribution of input quantum states, U_j . The target operator is either U_{open} or U_{closed} depending of the state of the control qubits, which is encoded in the initial density matrix $\rho(0)$. By solving the Lindblad master equation, Eq. (5) we obtain the density matrix at a later time, $\rho(t)$. This is done using the Python toolbox QuTiP [32]. Having obtained the full density matrix we can then trace out the control degrees of freedom, yielding the desired quantum map $\mathcal{E}_t(\rho(0)) = \text{Tr}_T(\rho(t))$. We chose the basis, U_j of the average fidelity as all two-qubit Pauli operators on the form $(\sigma_1^x)^k (\sigma_1^z)^l (\sigma_N^x)^m (\sigma_N^z)^n$ for all combinations of $k, l, m, n \in \{0, 1\}$.

Thus given a set of model parameters the average fidelity can be calculated as a function of time for both set of gate configurations. In the case of the open gate, i.e. configuration $|0\rangle_C$, the average fidelity rises from some initial value to a maximum (unity for the perfect gate) at the gate time, which we denote t_g . Analytically we

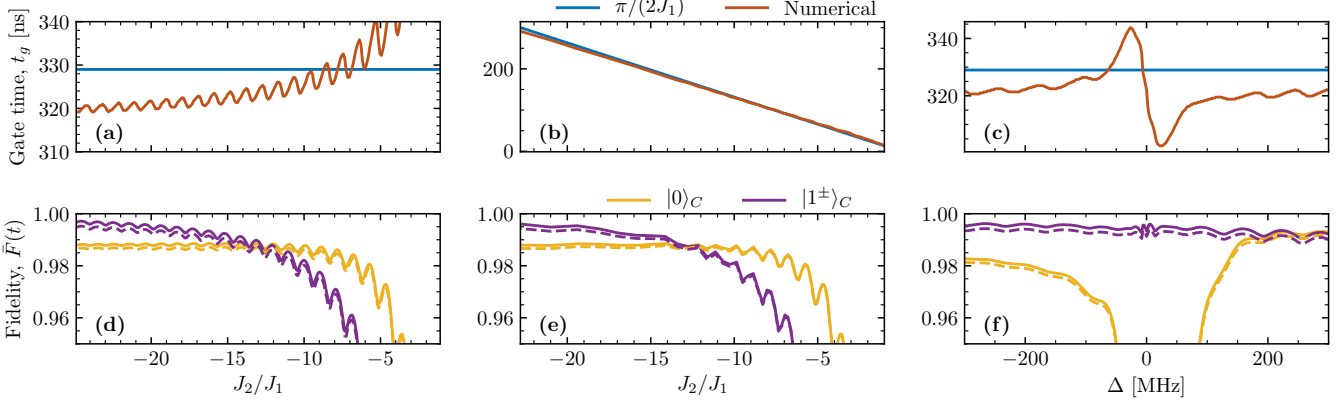


Figure 1. (a)-(c) Gate time as a function of the model parameters J_2 , $1/J_1$, and Δ . The blue lines indicates the analytical result of Eq. (7) and the red lines indicates the point of maximum average fidelity. (d)-(e) Average fidelities at the numerical gate time as a function of the model parameters J_2 , $1/J_1$, and Δ , both with (dashed lines) and without (solid lines) decoherence noise. The yellow lines indicates the fidelity when the gate is in the open configuration, while the purple line indicates that it is in the closed configuration.

expect this to be (see Appendix 1 b for a derivation of this)

$$t_g = \frac{\pi}{|2J_1|}, \quad (7)$$

however, for the simulations we find the best gate time numerically. In the case of the closed gate, i.e. the configuration $|1\rangle_C$, the average fidelity is initially unity and deviates only from this value due to leakage to the control qubits or as a result of decoherence noise.

In order to investigate the sensitivity of the parameter space we vary the parameters J_1 , J_2 , and Δ and show the gate time and average fidelities at the gate time in Fig. 1. The simulation is done both with and without noise. In Fig. 1(a) and (d) we vary the coupling of the control qubits, $J_2 \equiv J_2^x = J_2^z$, in the configuration $|1^\pm\rangle_C$, while keeping the remaining coupling constants at $J_1 = 30$ MHz. From this simulation we observe that the numerical gate time is about 5% faster than the analytical, and for large J_2/J_1 we observe almost unity average fidelity for the closed configuration of the gate, and between 0.98 and 0.99 for the open configuration. In Fig. 1(b) and (e) we vary the coupling between the target qubits and the control qubits, i.e. J_1 , while keeping the coupling between the control qubits constant at $J_2 = 750$ MHz, in the configuration $|1^\pm\rangle_C$. Again we observe a slightly shorter numerical gate time, and fidelities of close to unity and just between 0.98 and 0.99 for the closed and open configuration respectively. In Fig. 1(c) and (f) we vary J_2^x and keeping $J_2^z = 600$ MHz in the case of the gate being in the configuration $|1^\pm\rangle_C$ in order to effectively vary Δ around zero. We observe that the gate completely fails around zero, as it should, but we also conclude that we achieve a larger average fidelity (just above 0.99) for a positive detuning i.e. $J_2^z > J_2^x$, rather than a negative detuning. However for the case of $|1^\pm\rangle_C$ we find that the average fidelity is slightly larger when $J_2^z < J_2^x$. From the simulations we also find that a

different sign on the couplings J_1 and J_2 yields a slightly larger average fidelity.

The above mentioned simulations begs the question why the average gate fidelities does not approach unity, even when the requirements mentioned in Section II A are fulfilled? The answer to this question is found together with the answer to why the numerical gate time is shorter than the analytical gate time in Eq. (7). It all comes down to the fact that even though the state $|1\rangle|0\rangle_C|1\rangle$ is indeed an eigenstate of the Hamiltonian, it is also degenerate with the states $|1\rangle|1^\pm\rangle_C|0\rangle$ and $|0\rangle|1^\pm\rangle_C|1\rangle$ depending on the choice of Δ_\pm (note that these states are not the same as the configurations of the closed gate). This means that the system will oscillate between these three states, in a manner similar to how the open gate oscillates between states with a single excitation. However, the time scale for the oscillation of the double excitation is less than for the single excitation, with an oscillation time of about 90% of the analytical gate time. This means that some time between $0.9t_g$ and t_g we will observe maximum average fidelity, less unity, depending on the configuration of the system.

This does, however, not mean that it is impossible to achieve perfect transfer for some states, in a well configured system. Namely as long as not *both* the input and output qubit are in a superposition state, the state is transferred perfectly, when disregarding decoherence noise.

Note that the resonance of the eigenstates mentioned above is the same resonance that makes the gate work to begin with, in that case it is the states $|1\rangle|0\rangle_C|0\rangle$, $|0\rangle|0\rangle_C|1\rangle$, and $|0\rangle|1^\pm\rangle_C|0\rangle$ that are in resonance.

III. POSSIBLE PHYSICAL REALIZATION

We wish to implement the Hamiltonian in Eq. (3), and thus the swapping gate, using superconducting circuits.

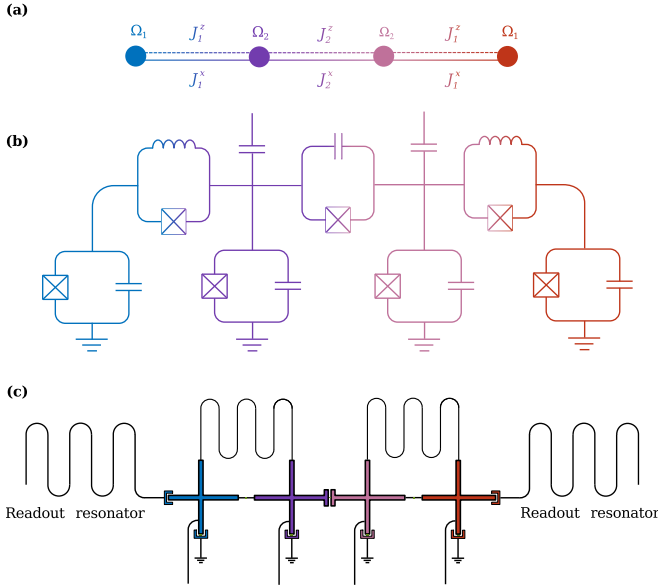


Figure 2. (a) The desired spin model as seen in Eq. (3). (b) The lumped circuit model for the super conducting circuit used to implement the above system. The crossed boxes represent Josephson junctions, the parallel lines capacitors, and the curled wires inductors. (c) Possible circuit design, consisting of four X-mon style superconducting islands, all grounded and with control lines from below. The small green patches indicates Josephson junctions, while the bend wires represent inductors. The first and last qubits are connected to an readout resonator as well. The colors indicates with parts of the three model that corresponds to each other.

As in the previous section we will focus on implementing the case of $N = 4$, but the idea is easily expanded to larger N .

A. Superconducting circuit

The circuit used to implement the system can be seen in Fig. 2(b). The circuit consists of four transmon type qubits [38], which are all grounded and connected in series through Josephson junctions, with as small of a parasitic capacitance as possible. In parallel with the connecting Josephson junctions is either a capacitor or an inductor, alternating between these two. Additional qubits are added to the chain by connecting them through a Josephson junction and either a capacitor or an inductor. It is important that two connecting capacitance are not next to each other, since this will induce cross talk between the nodes. When there are only a capacitor between every other pair of nodes the capacitance matrix becomes block diagonal, which means that its inverse will be block diagonal as well. However, had there been capacitors between all nodes the capacitance matrix would have been tridiagonal, and its inverse not necessarily be tridiagonal, which possibly yields cross talk, i.e. couplings other than nearest neighbor coupling. In reality there will always

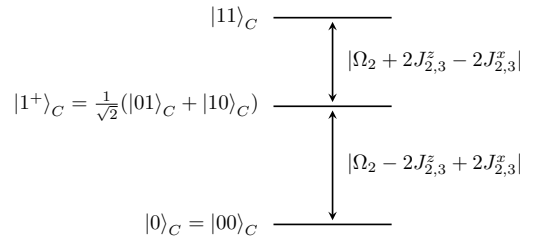


Figure 3. Sketch of the state of the control qubits.

be a parasitic capacitance between two nodes connected through a Josephson junction, however, not including these are equivalent to assuming $C_i \gg C_{i,i+1}$ where C_i is the shunting capacitance of the i th qubit and $C_{i,i+1}$ is the parasitic capacitance between the i th and $(i+1)$ th node. See Appendix 6 for a discussion on the emergence of cross talk due to capacitive couplings.

Instead of transmon qubits one could, in principle, have used other types of superconducting qubits such as the C-shunted qubit (or floxmons) [33–37], or fluxonium [39].

For each node in the circuit we have a related flux degree of freedom, which we denote ϕ_i [40]. Interactions between the qubits are induced by capacitors and inductors, which induce XX couplings, and Josephson junctions which induce both XX and ZZ couplings. A detailed calculation going from the circuit design to the Hamiltonian in Eq. (3) can be found in Appendix 3.

In order to operate the gate successively, we need a scheme for preparing the state of the gate. We would like to be able to address the control qubits exclusively, i.e. opening and closing the gate independently of the target qubits. This is possible when the target qubits are detuned from the control qubits, i.e. Δ is sufficiently large, compared to the couplings between the control qubits and the target qubits. A large detuning can, in experiments, be obtained by tuning the external fluxes.

We can achieve control of the gate by driving the middle nodes. The driving is performed by adding an external field to the nodes through capacitors. The control lines are depicted on Fig. 7(c) as the wires left of the ground. This introduces an extra driving term to the Hamiltonian which in the interaction picture takes the form

$$H_d(t) = \frac{A}{2} I(t) [(\sigma_2^y + \sigma_3^y) \sin \delta t - (\sigma_2^x + \sigma_3^x) \cos \delta t], \quad (8)$$

for an in-phase driving, where we have defined $\delta = \omega - \Omega_1$, ω is the driving frequency, and $I(t)$ is the envelope of the driving pulse. Like the rest of the Hamiltonian this term preserves the total spin of the two gate qubits, hence it does not mix the singlet and triplet states. We can therefore ignore the singlet state $|1^-\rangle_C$, when starting from any of the triplet states shown in Fig. 3.

Rabi oscillations between the closed and open states are then generated by the driving, provided the driving frequency matches the energy difference $\omega = |\Omega - 2J_{2,3}^z + 2J_{2,3}^x|$ and $A \ll J_{2,3}^z$. A π -pulse would then shift between

the $|0\rangle_C$ and $|1^+\rangle_C$ states in a few microseconds depending on the size of A . The energy difference between the open or closed states and the last state $|11\rangle_C$ are far enough from ω such that we do not populate this state by accident. Thus using this scheme we can drive between an open and closed gate using merely an external microwave drive. For a detailed calculation of the driving force see Appendix 4.

If we were to drive the system for an intermediate time between 0 and one π -pulse, we would obtain a superposition of the open and closed gate. Suppose that we drive the Rabi oscillation for half a π -pulse, $t = \pi/2A$, in this case we would get the superposition

$$|1^+\rangle_C \rightarrow \frac{1}{\sqrt{2}} (|1^+\rangle_C + i|0\rangle_C). \quad (9)$$

In this case the gate would permit a superposition of the system being transferred and not. In the same way that the transferred state accumulates a phase during the transfer so does the superposition gate. The phase obtained by the superposition gate is simply the energy difference between the open and closed state. Thus we must include a phase factor of

$$e^{-i(\Omega_2 - 2J_{2,3}^z + 2J_{2,3}^x)t}, \quad (10)$$

on the gate when evaluating the state.

A lumped circuit diagram is not enough for a possible realistic implementation and we therefore propose an experimental realistic chip design, which can be seen in Fig. 2(c). The chip consists of four X-mon like superconducting islands [41], each connected to the ground through a transmon qubit, and each connected to a control line. All qubits are connected to its neighbor through a Josephson junction, and the two middle are close to one another in order to create a capacitive coupling, while the outer islands are farther from the middle islands in order to minimize the capacitive coupling, while being connected through an inductor each. The outer islands corresponds to the target qubits and are therefore connected to an LC -resonator each, in order to be able to perform measurements on them. The two middle islands corresponds to the control qubits.

B. Leakage and infidelities

Due to the fact that we require a large coupling coefficient between the two control qubits, J_2 , the superconducting circuit is vulnerable to leakage to higher excited states than the two lowest states. In order to investigate the amount of leakage in our system we simulate it with the control qubits being qutrits, i.e. including the three lowest states of the system. The simulation is done for the realistic parameters: $J_1 = 30 \text{ MHz} \cdot 2\pi$, $J_2 = -500 \text{ MHz} \cdot 2\pi$, and an anharmonicity of $\mathcal{A}_2 = 300 \text{ MHz} \cdot 2\pi$. The average fidelity is shown in Fig. 4 together with the results for the system with purely qubits.

From Fig. 4 we observe that the average fidelity is not affected significantly in the large picture, however, if we

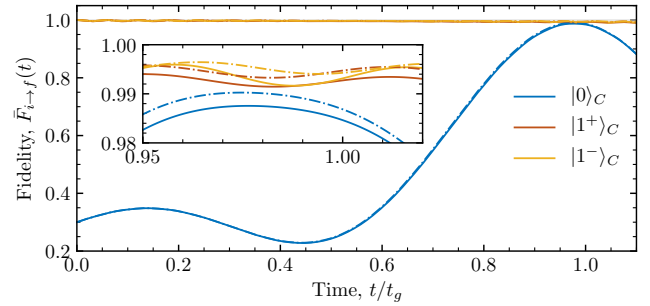


Figure 4. Average fidelity of the system with realistic parameters as a function of time. The simulations is done both for control qubits (solid lines) and qutrits (dashed dotted lines). The average fidelity is plotted for all possible configurations of the control qubits/qutrits. The insert shows a zoom of the peak of the average fidelity in the open configuration $|0\rangle_C$, i.e. around $t \sim t_g$.

zoom in on the peak of the average fidelity in the open state we observe that the average fidelity has indeed increase to above 0.99, contrary to an expected decrease. This is due to the fact that the inclusion of the second excited states changes the resonance of the states $|1\rangle|0\rangle_C|1\rangle$, $|1\rangle|1^\mp\rangle_C|0\rangle$, and $|0\rangle|1^\mp\rangle_C|1\rangle$ into an approximate resonance, yielding a slower period of oscillation, which brings it closer to the gate time t_g and thus increasing the fidelity at the gate time.

Besides leakage to higher excited states capacitive couplings beyond nearest neighbor qubits posses the biggest treat to gate fidelity. We therefore consider the effect of cross talk on the average gate fidelities as seen in Fig. 5. From the simulation we see that next-to-nearest couplings have no effect on the gate when it is in its closed configurations $|1^\pm\rangle_C$, and only have little effect when it is in its open configuration $|0\rangle_C$. In fact the average fidelity increases a tiny amount until the next-to-nearest neighbor coupling is 3% of the nearest neighbor coupling between the target qubits and the control qubits. This is consistent with the result of Ref. [42]. Next-to-next-to-nearest couplings, on the other hand, have a much more significant influence on the system when the coupling strength is above 2% of the target-control coupling, and we conclude that the gate fidelity decreases as the square of the next-to-next-to-nearest coupling strength. This is expected since the next-to-next-to-nearest coupling is a direct coupling of the input and output qubits.

IV. EXTENSIONS AND OUTLOOK

Besides being used for the above mentioned swapping gate, the superconducting circuit is interesting in many other settings due to the fact that it implements the most fundamental of all spin model structures: the linear spin chain. The linear chain is the obvious choice for a “quantum wire” in an implementation of quantum information

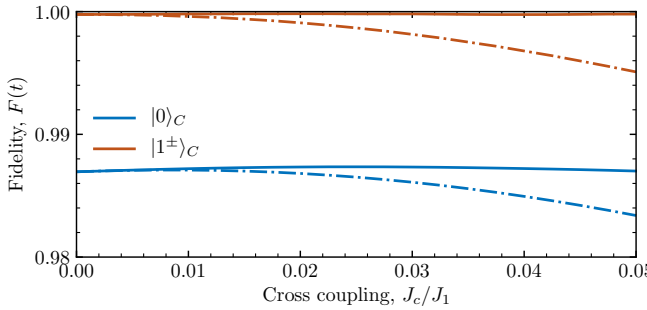


Figure 5. Average fidelities of the control qubits in both states for increasing strength of coupling beyond nearest neighbor coupling, J_c . The solid lines is with next-to-nearest couplings included, and the dashed dotted lines are with up to next-to-next-to-nearest neighbor coupling.

processing, especially if configured for perfect state transfer over a fixed period of time [43]. The superconducting circuit in Fig. 2 is a possible candidate for this application due to its straight-forward scaling.

Consider the case where we want a model without any ZZ couplings. One way to achieve this is simply to fine tune the system and thus suppressing these. However, there is an easier way: All the contribution to the ZZ coupling stems from the Josephson junctions, and thus removing those will create a purely XX coupled spin chain. One could even remove the capacitors and just couple the qubits through a series of inductors similar to the chain in Ref. [44] or the *1D Tight-Binding Lattice for Photons* mentioned in Ref. [45], but with superconducting qubit instead of LC -resonators in order to create a spin model and not a boson model. This circuit could also be used to investigate the Su-Schrieffer-Heeger (SSH) model [46, 47] defined on the dimerized one-dimensional lattice with two sites per unit cell, both in the strong and weak coupling limit in relation the the Zak phase as considered by Ref. [48]. It should be mentioned that we were not able to reproduce the lattice in Ref. [48] using their suggested circuit due to the before mentioned fact that the inverse of the capacitance matrix, with couplings entirely with capacitors, is not tridiagonal, which induces non-negligible cross talk, especially in the strong coupling limit. The occurrence of this problem is illuminated in Appendix 6. Our circuit does not introduce this cross talk, and is therefore more suitable for the investigation of the SSH model.

The superconducting circuit presented here can also

easily be molded into a box model where each qubit corresponds to a corner of the box and each edge a coupling. This is done simply by connecting the first and last coupling with a Josephson junction and/or a capacitor depending on which kind of coupling one wishes to implement. Such a system could be used to engineering quantum spin liquids and many-body Majorana states [49].

Lastly we mention that even though we have tried to avoid cross talk up until now, it is possible to modify the circuit into having all-to-all XX couplings by connecting all superconducting islands with capacitors. The most effective implementation of this would be in the box shape, since this avoids the use of 3D integration [50, 51]. For all-to-all ZZ couplings one would have to use 3D integration as all superconducting islands must be connected directly via a Josephson junction.

V. CONCLUSION

We have investigated a linear chain of qubits and found that under the right configuration these can operate as a two-qubit swapping gate with different phases depending on the initial conditions. In particular we have focused on the case of four qubits and shown that it can create a a swapping gate with a fidelity around 0.99, even when including realistic decoherence noise and leakage to higher excited states.

Furthermore we have proposed a superconducting circuit which realizes the four qubit spin chain. Both a lumped circuit model and a possible chip design using Xmon style qubits have been presented and we have discussed how to operate this circuit between the different configurations of a given gate. Finally, we have discussed how the superconducting circuit can be modified in a simple manner to realize other models with Hamiltonians that have attracted considerable interest in recent times. This shows that the basic model and layout we propose may have extended utility in both quantum processing and quantum simulation research directions.

ACKNOWLEDGMENTS

The authors would like to thank T. Bækkegaard, L. B. Kristensen, and N. J. S. Loft for discussion on different aspects of the work. This work is supported by the Danish Council for Independent Research and the Carlsberg Foundation.

[1] D. P. DiVincenzo, *Phys. Rev. A* **51**, 1015 (1995).
[2] I. Buluta, S. Ashhab, and F. Nori, *Reports on Progress in Physics* **74**, 104401 (2011).
[3] S. Gustavsson, O. Zwier, J. Bylander, F. Yan, F. Yoshihara, Y. Nakamura, T. P. Orlando, and W. D. Oliver, *Phys. Rev. Lett.* **110**, 040502 (2013).
[4] M. Reagor, C. B. Osborn, N. Tezak, A. Staley, G. Prawiroatmodjo, M. Scheer, N. Alidoust, E. A. Sete,

N. Didier, M. P. da Silva, E. Acalá, J. Angeles, A. Bestwick, M. Block, B. Bloom, A. Bradley, C. Bui, S. Caldwell, L. Capelluto, R. Chilcott, J. Cordova, G. Crossman, M. Curtis, S. Deshpande, T. El Bouayadi, D. Girshovich, S. Hong, A. Hudson, P. Karalekas, K. Kuang, M. Lenihan, R. Manenti, T. Manning, J. Marshall, Y. Mohan, W. O'Brien, J. Otterbach, A. Papageorge, J.-P. Paquette, M. Pelstring, A. Polloreno, V. Rawat, C. A. Ryan, R. Renzas, N. Rubin, D. Russel, M. Rust, D. Scarabelli, M. Selvanayagam, R. Sinclair, R. Smith, M. Suska, T.-W. To, M. Vahidpour, N. Vodrahalli, T. Whyland, K. Yadav, W. Zeng, and C. T. Rigetti, *Science Advances* **4** (2018), 10.1126/sciadv.aao3603.

[5] M. A. Rol, C. C. Bultink, T. E. O'Brien, S. R. de Jong, L. S. Theis, X. Fu, F. Luthi, R. F. L. Vermeulen, J. C. de Sterke, A. Bruno, D. Deurloo, R. N. Schouten, F. K. Wilhelm, and L. DiCarlo, *Phys. Rev. Applied* **7**, 041001 (2017).

[6] S. Sheldon, E. Magesan, J. M. Chow, and J. M. Gambetta, *Phys. Rev. A* **93**, 060302 (2016).

[7] Z. Chen, J. Kelly, C. Quintana, R. Barends, B. Campbell, Y. Chen, B. Chiaro, A. Dunsworth, A. G. Fowler, E. Lucero, E. Jeffrey, A. Megrant, J. Mutus, M. Neeley, C. Neill, P. J. J. O'Malley, P. Roushan, D. Sank, A. Vainsencher, J. Wenner, T. C. White, A. N. Korotkov, and J. M. Martinis, *Phys. Rev. Lett.* **116**, 020501 (2016).

[8] R. Barends, J. Kelly, A. Megrant, A. Veitia, D. Sank, E. Jeffrey, T. C. White, J. Mutus, A. G. Fowler, B. Campbell, Z. Chen, Y. Chen, B. Chiaro, A. Dunsworth, C. Neill, P. O'Malley, P. Roushan, A. Vainsencher, J. Wenner, A. N. Korotkov, A. N. Cleland, and J. M. Martinis, *Nature* **508**, 500 (2014).

[9] R. Raussendorf and J. Harrington, *Phys. Rev. Lett.* **98**, 190504 (2007).

[10] A. D. Córcoles, E. Magesan, S. J. Srinivasan, A. W. Cross, M. Steffen, J. M. Gambetta, and J. M. Chow, *Nature Communications* **6**, 6979 (2015).

[11] T. E. O'Brien, B. Tarasinski, and L. DiCarlo, *npj Quantum Information* **3**, 39 (2017).

[12] A. G. Fowler, M. Mariantoni, J. M. Martinis, and A. N. Cleland, *Phys. Rev. A* **86**, 032324 (2012).

[13] J. Kelly, R. Barends, B. Campbell, Y. Chen, Z. Chen, B. Chiaro, A. Dunsworth, A. G. Fowler, I.-C. Hoi, E. Jeffrey, A. Megrant, J. Mutus, C. Neill, P. J. J. O'Malley, C. Quintana, P. Roushan, D. Sank, A. Vainsencher, J. Wenner, T. C. White, A. N. Cleland, and J. M. Martinis, *Phys. Rev. Lett.* **112**, 240504 (2014).

[14] Y. Chen, C. Neill, P. Roushan, N. Leung, M. Fang, R. Barends, J. Kelly, B. Campbell, Z. Chen, B. Chiaro, A. Dunsworth, E. Jeffrey, A. Megrant, J. Y. Mutus, P. J. J. O'Malley, C. M. Quintana, D. Sank, A. Vainsencher, J. Wenner, T. C. White, M. R. Geller, A. N. Cleland, and J. M. Martinis, *Phys. Rev. Lett.* **113**, 220502 (2014).

[15] S. Sheldon, L. S. Bishop, E. Magesan, S. Filipp, J. M. Chow, and J. M. Gambetta, *Phys. Rev. A* **93**, 012301 (2016).

[16] D. C. McKay, S. Filipp, A. Mezzacapo, E. Magesan, J. M. Chow, and J. M. Gambetta, *Phys. Rev. Applied* **6**, 064007 (2016).

[17] A. Dewes, F. R. Ong, V. Schmitt, R. Lauro, N. Boulant, P. Bertet, D. Vion, and D. Esteve, *Phys. Rev. Lett.* **108**, 057002 (2012).

[18] Y. Salathé, M. Mondal, M. Oppliger, J. Heinsoo, P. Kurpiers, A. Potočnik, A. Mezzacapo, U. Las Heras, L. Lamata, E. Solano, S. Filipp, and A. Wallraff, *Phys. Rev. X* **5**, 021027 (2015).

[19] S. Poletto, J. M. Gambetta, S. T. Merkel, J. A. Smolin, J. M. Chow, A. D. Córcoles, G. A. Keefe, M. B. Rothwell, J. R. Rozen, D. W. Abraham, C. Rigetti, and M. Steffen, *Phys. Rev. Lett.* **109**, 240505 (2012).

[20] H. Paik, A. Mezzacapo, M. Sandberg, D. T. McClure, B. Abdo, A. D. Córcoles, O. Dial, D. F. Bogorin, B. L. T. Plourde, M. Steffen, A. W. Cross, J. M. Gambetta, and J. M. Chow, *Phys. Rev. Lett.* **117**, 250502 (2016).

[21] M. Vojta, *Reports on Progress in Physics* **66**, 2069 (2003).

[22] C.-K. Hu, *Phys. Rev. B* **29**, 5103 (1984).

[23] K. Morita, T. Sugimoto, S. Sota, and T. Tohyama, *Phys. Rev. B* **97**, 014412 (2018).

[24] S. Depenbrock, I. P. McCulloch, and U. Schollwöck, *Phys. Rev. Lett.* **109**, 067201 (2012).

[25] O. V. Marchukov, A. G. Volosniev, M. Valiente, D. Petrosyan, and N. T. Zinner, *Nature Communications* **7**, 13070 (2016).

[26] M. Möttönen, J. J. Vartiainen, V. Bergholm, and M. M. Salomaa, *Phys. Rev. Lett.* **93**, 130502 (2004).

[27] M. Möttönen, J. J. Vartiainen, V. Bergholm, and M. M. Salomaa, “Transformation of quantum states using uniformly controlled rotations,” (2005), arXiv:quant-ph/0407010.

[28] R. Babbush, C. Gidney, D. W. Berry, N. Wiebe, J. McClean, A. Paler, A. Fowler, and H. Neven, *Phys. Rev. X* **8**, 041015 (2018).

[29] P. Zanardi, C. Zalka, and L. Faoro, *Phys. Rev. A* **62**, 030301 (2000).

[30] Z. Wang, S. Shankar, Z. K. Minev, P. Campagne-Ibarcq, A. Narla, and M. H. Devoret, “Cavity attenuators for superconducting qubits,” (2018), arXiv:1807.04849.

[31] M. A. Nielsen, *Physics Letters A* **303**, 249 (2002).

[32] J. R. Johansson, P. D. Nation, and F. Nori, *Comp. Phys. Comm.* **184**, 1234 (2013).

[33] T. P. Orlando, J. E. Mooij, L. Tian, C. H. van der Wal, L. S. Levitov, S. Lloyd, and J. J. Mazo, *Phys. Rev. B* **60**, 15398 (1999).

[34] J. E. Mooij, T. P. Orlando, L. Levitov, L. Tian, C. H. van der Wal, and S. Lloyd, *Science* **285**, 1036 (1999).

[35] C. H. van der Wal, A. C. J. ter Haar, F. K. Wilhelm, R. N. Schouten, C. J. P. M. Harmans, T. P. Orlando, S. Lloyd, and J. E. Mooij, *Science* **290**, 773 (2000).

[36] J. Q. You, X. Hu, S. Ashhab, and F. Nori, *Phys. Rev. B* **75**, 140515 (2007).

[37] F. Yan, S. Gustavsson, A. Kamal, J. Birenbaum, A. P. Sears, D. Hoyer, T. J. Gudmundsen, D. Rosenberg, G. Samach, S. Weber, J. L. Yoder, T. P. Orlando, J. Clarke, A. J. Kerman, and W. D. Oliver, *Nature Communications* **7**, 12964 (2016).

[38] J. Koch, T. M. Yu, J. Gambetta, A. A. Houck, D. I. Schuster, J. Majer, A. Blais, M. H. Devoret, S. M. Girvin, and R. J. Schoelkopf, *Phys. Rev. A* **76**, 042319 (2007).

[39] V. E. Manucharyan, J. Koch, L. I. Glazman, and M. H. Devoret, *Science* **326**, 113 (2009).

[40] U. Vool and M. H. Devoret, *International Journal of Circuit Theory and Applications* **45**, 897 (2017).

[41] R. Barends, J. Kelly, A. Megrant, D. Sank, E. Jeffrey, Y. Chen, Y. Yin, B. Chiaro, J. Mutus, C. Neill, P. O'Malley, P. Roushan, J. Wenner, T. C. White, A. N. Cleland, and J. M. Martinis, *Phys. Rev. Lett.* **111**, 080502 (2013).

[42] N. J. S. Loft, M. Kjaergaard, L. B. Kristensen,

C. K. Andersen, T. W. Larsen, S. Gustavsson, W. D. Oliver, and N. T. Zinner, “High-fidelity conditional two-qubit swapping gate using tunable ancillas,” (2018), [arXiv:1809.09049](https://arxiv.org/abs/1809.09049).

[43] M. Christandl, N. Datta, A. Ekert, and A. J. Landahl, *Phys. Rev. Lett.* **92**, 187902 (2004).

[44] C. Neill, P. Roushan, K. Kechedzhi, S. Boixo, S. V. Isakov, V. Smelyanskiy, A. Megrant, B. Chiaro, A. Dunsworth, K. Arya, R. Barends, B. Burkett, Y. Chen, Z. Chen, A. Fowler, B. Foxen, M. Giustina, R. Graff, E. Jeffrey, T. Huang, J. Kelly, P. Klimov, E. Lucero, J. Mutus, M. Neeley, C. Quintana, D. Sank, A. Vainsencher, J. Wenner, T. C. White, H. Neven, and J. M. Martinis, *Science* **360**, 195 (2018).

[45] J. Ningyuan, C. Owens, A. Sommer, D. Schuster, and J. Simon, *Phys. Rev. X* **5**, 021031 (2015).

[46] W. P. Su, J. R. Schrieffer, and A. J. Heeger, *Phys. Rev. Lett.* **42**, 1698 (1979).

[47] A. J. Heeger, S. Kivelson, J. R. Schrieffer, and W. P. Su, *Rev. Mod. Phys.* **60**, 781 (1988).

[48] T. Goren, K. Plekhanov, F. Appas, and K. Le Hur, *Phys. Rev. B* **97**, 041106 (2018).

[49] F. Yang, L. Henriet, A. Soret, and K. Le Hur, *Phys. Rev. B* **98**, 035431 (2018).

[50] D. Rosenberg, D. Kim, R. Das, D. Yost, S. Gustavsson, D. Hover, P. Krantz, A. Melyville, L. Racz, G. O. Samach, S. J. Weber, F. Yan, J. L. Yoder, A. J. Kerman, and W. D. Oliver, *npj Quantum Information* **3** (2017), <https://doi.org/10.1038/s41534-017-0044-0>.

[51] Y. Lu, N. Jia, L. Su, C. Owens, G. Juzeliunas, D. I. Schuster, and J. Simon, “Probing the berry curvature and fermi arcs of a weyl circuit,” (2018), [arXiv:1807.05243](https://arxiv.org/abs/1807.05243).

[52] D. Nield, *SIAM Review* **36**, 649 (1994).

[53] M. H. Devoret, in *Fluctuations Quantiques/Quantum Fluctuations: Les Houches Session LXIII*, edited by S. Reynaud, E. Giacobino, and J. Zinn-Justin (Elsevier, 1997) p. 351.

[54] G. Wendin and V. Shumeiko, (2005), [arXiv:cond-mat/0508729](https://arxiv.org/abs/cond-mat/0508729).

[55] W. S. Warren, *The Journal of Chemical Physics* **81**, 5437 (1984), <https://doi.org/10.1063/1.447644>.

[56] M. Steffen, J. M. Martinis, and I. L. Chuang, *Phys. Rev. B* **68**, 224518 (2003).

[57] J. M. Gambetta, F. Motzoi, S. T. Merkel, and F. K. Wilhelm, *Phys. Rev. A* **83**, 012308 (2011).

[58] F. Motzoi and F. K. Wilhelm, *Phys. Rev. A* **88**, 062318 (2013).

[59] P. Rebentrost and F. K. Wilhelm, *Phys. Rev. B* **79**, 060507 (2009).

[60] N. Khaneja, T. Reiss, C. Kehlet, T. Schulte-Herbrüggen, and S. J. Glaser, *Journal of Magnetic Resonance* **172**, 296 (2005).

[61] F. Motzoi, J. M. Gambetta, P. Rebentrost, and F. K. Wilhelm, *Phys. Rev. Lett.* **103**, 110501 (2009).

APPENDIX

1. The requirements for the gate

This appendix roughly follows the work of Ref. [25], but uses a different approach in some instances and includes a derivation of the requirement for perfect state transfer of superposition states. Consider a chain of N spin-1/2 particles described by a Heisenberg XXZ spin model as in Eq. (3) of the main text, with the same spatial symmetry requirements, i.e. $J_i^{x,z} = J_{N-i}^{x,z}$ and $\Delta_i = \Delta_{N-1-i}$.

a. Deriving the relevant eigenstates

Since the Hamilton in Eq. (3) preserves excitation we can consider the problem in each subspace, \mathcal{B}_k of total excitation, $k = 0, \dots, 4$. A closed state of a gate allows no dynamics, thus we require the state to be stationary. This is achieved by the eigenstate of the Hamiltonian. For the sake of completeness consider first the subspaces $\mathcal{B}_{0,4}$ these consist of only one state, $|0000\rangle$ or $|1111\rangle$, these are obviously the eigenstate of the system and stationary (since the Hamiltonian is preserves excitation we already knew this). The eigenenergies of these states are $E_{0,4} = \mp\Delta + J_2^z + 2J_1^z$, minus for E_0 and plus for E_4 .

Consider now the subspaces \mathcal{B}_1 consisting of the states $\{|1000\rangle, |0100\rangle, |0010\rangle, |0001\rangle\}$ (the subspace \mathcal{B}_3 works in an identical way just with every the excitation of every state exchanged, i.e. exchanging $0 \leftrightarrow 1$ in the states). In this basis the Hamiltonian matrix reads

$$H_1 = \begin{pmatrix} -\Delta + J_2^z & 2J_1^x & 0 & 0 \\ 2J_1^x & -J_2^z & 2J_2^x & 0 \\ 0 & 2J_2^x & -J_2^z & 2J_1^x \\ 0 & 0 & 2J_1^x & -\Delta + J_2^z \end{pmatrix}. \quad (11)$$

Now consider the last and largest subspace \mathcal{B}_2 consisting of the six states $\{|0011\rangle, |0101\rangle, |0110\rangle, |1001\rangle, |1010\rangle, |1100\rangle\}$. In this basis the Hamiltonian matrix reads

$$H_2 = \begin{pmatrix} 2J_1^z - J_2^z & 2J_2^x & 0 & 0 & 0 & 0 \\ 2J_2^x & -2J_1^z - J_2^z & 2J_1^x & 2J_1^x & 0 & 0 \\ 0 & 2J_1^x & -2J_1^z + J_2^z - \Delta & 0 & 2J_1^x & 0 \\ 0 & 2J_1^x & 0 & -2J_1^z + J_2^z + \Delta & 2J_1^x & 0 \\ 0 & 0 & 2J_1^x & 2J_1^x & -2J_1^z - J_2^z & 2J_2^x \\ 0 & 0 & 0 & 0 & 2J_2^x & 2J_1^z - J_2^z \end{pmatrix}. \quad (12)$$

Now we wish for the closed state to be a superposition of the the two middle qubits when they have one excitation combined, thus we require the following the two states to be eigenstates of the Hamiltonian

$$|\psi_1\rangle = \cos\theta|0100\rangle + \sin\theta|0010\rangle, \quad (13a)$$

$$|\psi_2\rangle = \cos\theta|1100\rangle + \sin\theta|1010\rangle. \quad (13b)$$

Thus applying the Hamiltonian to the states we obtain

$$H_1|\psi_1\rangle = \begin{pmatrix} 2J_1^x \cos\theta \\ -J_2^z \cos\theta + 2J_2^x \sin\theta \\ 2J_2^x \cos\theta - J_2^z \sin\theta \\ 2J_1^x \sin\theta \end{pmatrix} = b_1 \begin{pmatrix} 0 \\ \cos\theta \\ \sin\theta \\ 0 \end{pmatrix},$$

$$H_2|\psi_2\rangle = \begin{pmatrix} (2J_1^z - J_2^z) \cos\theta + 2J_2^x \sin\theta \\ 2J_2^x \cos\theta - (2J_1^z + J_2^z) \sin\theta \\ 2J_1^x \sin\theta \\ 2J_1^x \sin\theta \\ 0 \\ 0 \end{pmatrix} = b_2 \begin{pmatrix} \cos\theta \\ \sin\theta \\ 0 \\ 0 \\ 0 \\ 0 \end{pmatrix},$$

where the last equality is the eigenstate requirement. For these equations to be satisfied it is evident that $J_1 \ll J_2$ for both the x and z couplings. From the remaining equations we see that $\theta = \pm\pi/4$ (not surprising considering the symmetry of the problem). This yields $b_1 = b_2 = 2J_2^x - J_2^z$.

Having found two eigenstate for H_1 ($\theta = \pm\pi/4$), we make a unitary transformation to the basis where these are eigenstates using the transformation matrix

$$\mathcal{V} = \begin{pmatrix} 1 & 0 & 0 & 0 \\ 0 & \frac{1}{\sqrt{2}} & \frac{1}{\sqrt{2}} & 0 \\ 0 & \frac{1}{\sqrt{2}} & -\frac{1}{\sqrt{2}} & 0 \\ 0 & 0 & 0 & 1 \end{pmatrix}, \quad (14)$$

which yields

$$\tilde{H}_1 = \mathcal{V}^{-1} H_1 \mathcal{V} = \begin{pmatrix} -\Delta + J_2^z & \sqrt{2}J_1^x & \sqrt{2}J_1^x & 0 \\ \sqrt{2}J_1^x & 2J_2^x - J_2^z & 0 & \sqrt{2}J_1^x \\ \sqrt{2}J_1^x & 0 & -2J_2^x - J_2^z & -\sqrt{2}J_1^x \\ 0 & \sqrt{2}J_1^x & -\sqrt{2}J_1^x & -\Delta + J_2^z \end{pmatrix}, \quad (15)$$

from which we realize that the last two eigenstate are the original two states $|1000\rangle$ and $|0001\rangle$, when J_1 is small. Spin transfer can be obtained if three of the levels are in resonance with each other. This can be obtained if $\Delta = \Delta_{\pm} = 2(J_2^z \pm J_2^x)$.

Now we need to consider the remaining subspace \mathcal{B}_2 to see if either of the eigenstates here are resonant. Therefore let

$$|\psi_{\pm}\rangle = \frac{1}{\sqrt{2}} (|01\rangle \pm |10\rangle), \quad (16)$$

and consider the basis $\{|0\psi_{-1}\rangle, |0\psi_{+1}\rangle, |0110\rangle, |1001\rangle, |1\psi_{-0}\rangle, |1\psi_{+0}\rangle\}$, which we transform into using

$$\mathcal{V} = \begin{pmatrix} \frac{1}{\sqrt{2}} & \frac{1}{\sqrt{2}} & 0 & 0 & 0 & 0 \\ \frac{1}{\sqrt{2}} & -\frac{1}{\sqrt{2}} & 0 & 0 & 0 & 0 \\ 0 & 0 & 1 & 0 & 0 & 0 \\ 0 & 0 & 0 & 1 & 0 & 0 \\ 0 & 0 & 0 & 0 & \frac{1}{\sqrt{2}} & \frac{1}{\sqrt{2}} \\ 0 & 0 & 0 & 0 & \frac{1}{\sqrt{2}} & -\frac{1}{\sqrt{2}} \end{pmatrix}, \quad (17)$$

which yields the Hamiltonian

$$\tilde{H}_2 = \begin{pmatrix} 2J_2^x - J_2^z & J_2^z & \sqrt{2}J_1^x & \sqrt{2}J_1^x & 0 & 0 \\ J_2^z & -J_2^z - 2J_2^x & -\sqrt{2}J_1^x & -\sqrt{2}J_1^x & 0 & 0 \\ \sqrt{2}J_1^x & -\sqrt{2}J_1^x & -2J_1^z + J_2^z - \Delta & 0 & \sqrt{2}J_1^x & \sqrt{2}J_1^x \\ \sqrt{2}J_1^x & -\sqrt{2}J_1^x & 0 & -2J_1^z + J_2^z + \Delta & \sqrt{2}J_1^x & \sqrt{2}J_1^x \\ 0 & 0 & \sqrt{2}J_1^x & \sqrt{2}J_1^x & 2J_2^x - J_2^z & J_1^z \\ 0 & 0 & \sqrt{2}J_1^x & \sqrt{2}J_1^x & -J_1^z & -J_1^z - 2J_2^x \end{pmatrix}, \quad (18)$$

which is approximately diagonal for $J_1 \ll J_2$. Now we need to verify that the desired closed states $|1\psi_{\pm 0}\rangle$ is non-resonant with all the connected other states, and therefore do not evolve. The state has the eigenenergy

$$\tilde{E}_{1\psi_{\pm 0}} = \pm 2J_2^x - J_2^z. \quad (19)$$

Now assume $\Delta = \Delta_+$, then the states $|0110\rangle$ and $|1001\rangle$ obtain the eigenenergies

$$\tilde{E}_{0110} = -2J_1^z + J_2^z + \Delta_+ \simeq 3J_2^z + 2J_2^x, \quad (20)$$

$$\tilde{E}_{1001} = -2J_1^z + J_2^z - \Delta_+ \simeq -J_2^z + 2J_2^x, \quad (21)$$

which means that $|0\psi_{+1}\rangle$ is highly non-resonant with all connected states unless $J_2^z = 0$. Note that the state $|1\psi_{+0}\rangle$ have the same energy, but is not directly connected with $|0\psi_{+1}\rangle$. Note, however that the states $|0\psi_{-1}\rangle, |1\psi_{-0}\rangle$, and $|1001\rangle$ are resonant.

A similar argument can be made for Δ_- . Assume $\Delta = \Delta_-$, then the states $|0110\rangle$ and $|1001\rangle$ obtain the eigenenergies

$$\tilde{E}_{0110} = -2J_1^z + J_2^z + \Delta_- \simeq 3J_2^z - 2J_2^x, \quad (22)$$

$$\tilde{E}_{1001} = -2J_1^z + J_2^z - \Delta_- \simeq -J_2^z - 2J_2^x, \quad (23)$$

which means that $|0\psi_{-1}\rangle$ is highly non-resonant with all connected states unless $J_2^z = 0$. Note that the state $|1\psi_{-0}\rangle$ have the same energy, but is not directly connected with $|0\psi_{-1}\rangle$. Note, however that the states $|0\psi_{+1}\rangle, |1\psi_{+0}\rangle$, and $|1001\rangle$ are resonant. This means that the system will oscillate between these three states if started in any one of them. This presents a problem for the state $|1001\rangle$, which we would like to stay unchanged. However, it is not a problem if the period of oscillation between these three state are close to the gate time, since then the system will be in the desired state at the gate time.

Lastly we must also consider the state $|1\psi_{\pm 1}\rangle$, since we would like it to remain stationary. However, due to the symmetry of the system the subspace which it belongs to, \mathcal{B}_3 operates identically to the subspace \mathcal{B}_1 , and thus the state must behave identically to the states $|0\psi_{\pm 0}\rangle$, which is indeed stationary as discussed above.

b. *Transfer time*

In order to verify that perfect transfer is achieved and to find the transfer time, we wish to expand the initial and final states in the basis of eigenvectors in the original basis. Therefore we find the eigenvalues of Eq. (11) to be

$$E_1 = -J_2^x - \frac{1}{2}\Delta_{\pm} - \sqrt{4(J_1^x)^2 + \left(\frac{1}{2}\Delta_{\pm} - J_2^x - J_2^z\right)^2}, \quad (24a)$$

$$E_2 = J_2^x - \frac{1}{2}\Delta_{\pm} - \sqrt{4(J_1^x)^2 + \left(\frac{1}{2}\Delta_{\pm} + J_2^x - J_2^z\right)^2}, \quad (24b)$$

$$E_3 = -J_2^x - \frac{1}{2}\Delta_{\pm} + \sqrt{4(J_1^x)^2 + \left(\frac{1}{2}\Delta_{\pm} - J_2^x - J_2^z\right)^2}, \quad (24c)$$

$$E_4 = J_2^x - \frac{1}{2}\Delta_{\pm} + \sqrt{4(J_1^x)^2 + \left(\frac{1}{2}\Delta_{\pm} + J_2^x - J_2^z\right)^2}, \quad (24d)$$

and the corresponding non-normalized eigenvectors in the original basis are

$$|\Psi_1\rangle = \left\{ 1, \frac{4(J_1^x)^2 - 2J_2^x(2J_2^z - J_2^z + E_3)}{2J_1^x(J_2^z + E_1)}, \frac{J_2^z - 2J_2^x + E_3}{-2J_1^x}, 1 \right\}, \quad (25a)$$

$$|\Psi_2\rangle = \left\{ 1, \frac{4(J_1^x)^2 + 2J_2^x(2J_2^z + J_2^z - E_4)}{2J_1^x(J_2^z + E_2)}, \frac{J_2^z - 2J_2^x + E_4}{2J_1^x}, -1 \right\}, \quad (25b)$$

$$|\Psi_3\rangle = \left\{ 1, \frac{4(J_1^x)^2 - 2J_2^x(2J_2^z - J_2^z + E_1)}{2J_1^x(J_2^z + E_3)}, \frac{J_2^z - 2J_2^x + E_1}{-2J_1^x}, 1 \right\}, \quad (25c)$$

$$|\Psi_4\rangle = \left\{ 1, \frac{4(J_1^x)^2 + 2J_2^x(2J_2^z + J_2^z - E_2)}{2J_1^x(J_2^z + E_4)}, \frac{J_2^z - 2J_2^x + E_2}{2J_1^x}, -1 \right\}. \quad (25d)$$

We now expand the final and initial state in the basis of the eigenvectors above

$$|1000\rangle = \sum_{k=1}^4 a_k^{(i)} |\Psi_k\rangle, \quad (26a)$$

$$|0001\rangle = \sum_{k=1}^4 a_k^{(f)} |\Psi_k\rangle. \quad (26b)$$

Since the Hamiltonian of Eq. (11) is a bisymmetric matrix the expansion coefficients are related as $a_k^{(i)} = (-1)^k a_k^{(f)}$ [52]. We thus apply the time evolution operator $U(t) = e^{-iH_1 t}$ to the initial state in Eq. (26a), and by setting it equal to the final state in Eq. (26b) we obtain the following condition of perfect state transfer after t_f

$$\sum_{k=1}^4 [e^{-iE_k t_f} - (-1)^k] a_k^{(i)} |\Psi_k\rangle = 0. \quad (27)$$

and thus the conditions for perfect state transfer are

$$E_k t_f = \begin{cases} (2n_k + 1)\pi & \text{for } k = 1, 3, \\ 2n_k \pi & \text{for } k = 2, 4, \end{cases} \quad (28)$$

thus we find the sufficient conditions for the state $|1000\rangle$ to evolve into the state $|0001\rangle$ to be

$$|E_{k+1} - E_k| t_f = (2m_k + 1)\pi, \quad (29)$$

where m_k is an integer since we assume $E_1 < E_2 < E_3 < E_4$. For Δ_+ we find the energy distance between the equidistant levels to be

$$\begin{aligned}|E_2 - E_1| &= \left| 2J_1^x + 2J_2^x - \sqrt{(2J_1^x)^2 + (2J_2^x)^2} \right| \simeq |2J_1^x|, \\ |E_3 - E_2| &= \left| 2J_1^x - 2J_2^x + \sqrt{(2J_1^x)^2 + (2J_2^x)^2} \right| \simeq |2J_1^x|, \\ |E_4 - E_3| &= \left| -2J_1^x + 2J_2^x + \sqrt{(2J_1^x)^2 + (2J_2^x)^2} \right| \simeq |4J_2^x + 2J_1^x|.\end{aligned}$$

For $J_1^x \ll J_2^x$ we see the the three lowest levels are equidistant with the spacing $|2J_1^x|$, while the highest energy level is far above the others. Thus we can achieve nearly perfect state transfer for $t = \pi/|2J_1^x|$. A completely similar argument can be made for Δ_- .

Now consider the initial and final states

$$|i\rangle = a|1000\rangle + b|0000\rangle, \quad (30a)$$

$$|f\rangle = a|0001\rangle - b|0000\rangle, \quad (30b)$$

where $|a|^2 + |b|^2 = 1$. The change of sign on the last term is due to the fact that the eigenstate $|0000\rangle$ receives a phase factor of $e^{-i\pi} = -1$ during the transfer, as mentioned in the main text. Once again we expand the states $|1000\rangle$ and $|0001\rangle$ into the basis of eigenvectors of Eq. (25)

$$|i\rangle = a \sum_{k=1}^4 a_k^{(i)} |\Psi_k\rangle + b|0000\rangle, \quad (31a)$$

$$|f\rangle = a \sum_{k=1}^4 a_k^{(f)} |\Psi_k\rangle - b|0000\rangle, \quad (31b)$$

and once again we time evolve the initial state and set it equal to the final state, yielding the condition for perfect state transfer after time t_f

$$a \sum_{k=1}^4 [e^{-iE_k t_f} - (-1)^k] a_k^{(i)} |\Psi_k\rangle + b [e^{-iE_0 t_f} + 1] |0000\rangle = 0, \quad (32)$$

where the eigenenergy of the non-excited state is $E_0 = -\Delta_{\pm} + J_2^z + 2J_1^z$, which for the case of Δ_+ is $E_0 = -J_2^z - 2J_2^x + 2J_1^z$. Thus besides the original requirements in Eq. (28) we also find the requirement

$$E_0 t_f = (2n_0 + 1)\pi, \quad (33)$$

where n_0 is an integer. Since $|0000\rangle$ is completely unexcited and thus the lowest state we find the condition

$$|E_1 - E_0| t_f = 2m_- \pi, \quad (34)$$

where m_0 is a positive integer. We find the distance between the two energy levels

$$|E_1 - E_0| = |2J_1^x + 2J_1^z|. \quad (35)$$

Solving for the transfer time in Eq. (34) and choosing $m_0 = 1$ in order to obtain the fastest transfer time we find

$$t_f = \frac{2\pi}{|E_1 - E_0|} = \frac{\pi}{|J_1^x + J_1^z|}. \quad (36)$$

From this it is clear that in order to obtain a transfer of the $|0000\rangle$ state in the same time as the states of \mathcal{B}_1 we must require $J_1^x = J_1^z$.

2. The $N = 5$ case

With five qubits there are still just two interaction coefficients $J_1^{x,z}$ and $J_2^{x,z}$ due to the spatial symmetry, where we still require $J_1^{x,z} \ll J_2^{x,z}$, however, their are now three different qubit frequencies and thus two different detunings, $\Delta \equiv \Delta_2 = \Delta_4$ and Δ_3 . According to Ref. [25], in the basis of $\{|10000\rangle, |01000\rangle, |00100\rangle, |00010\rangle, |00001\rangle\}$ the eigenvalues of the Hamiltonian is

$$E_1 = \Delta + \frac{1}{2}\Delta_3 + 2J_2^z, \quad (37a)$$

$$E_+ \equiv E_2 = \frac{1}{2}\Delta + J_1^z - J_2^z + \sqrt{8(J_2^x)^2 + \left(\frac{1}{2}(\Delta - \Delta_3) + J_1^z - J_2^z\right)^2}, \quad (37b)$$

$$E_0 = E_3 = \frac{1}{2}\Delta_3, \quad (37c)$$

$$E_- \equiv E_4 = \frac{1}{2}\Delta + J_1^z - J_2^z - \sqrt{8(J_2^x)^2 + \left(\frac{1}{2}(\Delta - \Delta_3) + J_1^z - J_2^z\right)^2}, \quad (37d)$$

$$E_5 = \Delta + \frac{1}{2}\Delta_3 + 2J_2^z, \quad (37e)$$

with (non-normalized) corresponding eigenstates

$$|\Psi_1\rangle = \{1, 0, 0, 0, 0\}, \quad (38a)$$

$$|\Psi_2\rangle = \{0, J_2^x, \frac{1}{2}\Delta_3 - E_+, J_2^x, 0\}, \quad (38b)$$

$$|\Psi_3\rangle = \{0, 1, 0, -1, 0\}, \quad (38c)$$

$$|\Psi_4\rangle = \{0, J_2^x, \frac{1}{2}\Delta_3 - E_-, J_2^x, 0\}, \quad (38d)$$

$$|\Psi_5\rangle = \{0, 0, 0, 0, 1\}, \quad (38e)$$

$$(38f)$$

where in agreement with the main text we define the states of the middle control qubits as $|1^\pm\rangle_C = \{J_2^x, \frac{1}{2}\Delta_3 - E_\pm, J_2^x\}$ and $|1^0\rangle_C = \{1, 0, -1\}$ in the basis of $\{|100\rangle, |010\rangle, |001\rangle\}$, and lastly we still define $|0\rangle_C = \{0, 0, 0\}$ as the open configuration.

In order to achieve resonant transfer between the states $|10000\rangle$ and $|00001\rangle$ we must find values of the detuning such that on of $E_{\pm,0}$ is equal to $E_1 = E_2$. For the case of $E_0 = E_1$ we find $\Delta = 2J_2^z$ and any Δ_3 , and the transfer of excitation goes via the resonant state $|0\rangle|1^0\rangle_C|0\rangle$. In the case of $E_1 = E_\pm$ we find that

$$\Delta = -\frac{2(J_2^x)^2}{\frac{1}{2}\Delta_3 + 2J_2^z} + J_2^z, \quad (39)$$

where the transfer goes via the states $|0\rangle|1^\pm\rangle_C|0\rangle$ depending on the value of $\frac{1}{2}\Delta_3 + 2J_2^z$, going through $|0\rangle|1^+\rangle_C|0\rangle$ for $\frac{1}{2}\Delta_3 + 2J_2^z < 0$ and $|0\rangle|1^-\rangle_C|0\rangle$ for $\frac{1}{2}\Delta_3 + 2J_2^z > 0$.

With these requirements the chain of qubits will work as a transistor as described by Ref. [25], however it does not guaranty that it will work as a swapping gate in the same manner as for four qubits. This is due to the fact that the transfer time of the states $|10000\rangle$ and $|10001\rangle$ have to coincide as was the case with $N = 4$. In fact we find that only the case of $E_1 = E_0$, i.e. resonant transfer via the state $|1^0\rangle_C$ creates the negative swapping gate of Eq. (4) with a fidelity close to 0.99, and operating similar to the case of $N = 4$. The remaining two possible configurations of Eq. (39), does not create any kind of swapping gate with a fidelity over 0.9.

In the closed configuration of $|1^\pm\rangle_C$, we find that the total excitation remains stationary, as it should, however, we also observe that in the case of a superposition input we acquire an internal phase, depending on the exact configuration of the gate. In the closed configuration of $|1^0\rangle_C$, i.e. when the gate is configured according to Eq. (39), we do, however, not pick up such a phase.

3. In depth analysis of the circuit

Here follows an in depth derivation of the spin model resulting from the circuit in Fig. 2(b). The circuit is shown in Fig. 7 as well, with labels on each element. The calculation are done for $N = 4$, but can easily be expanded to larger

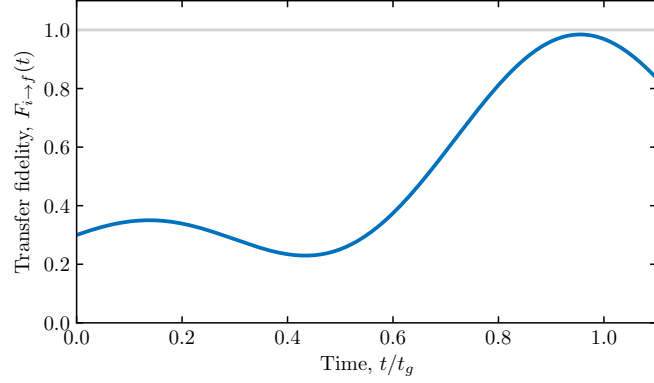


Figure 6. Average fidelity of the system with $N = 5$ qubits in the open configuration, i.e. $|0\rangle_C$, with resonant transfer via $|1^0\rangle_C$.

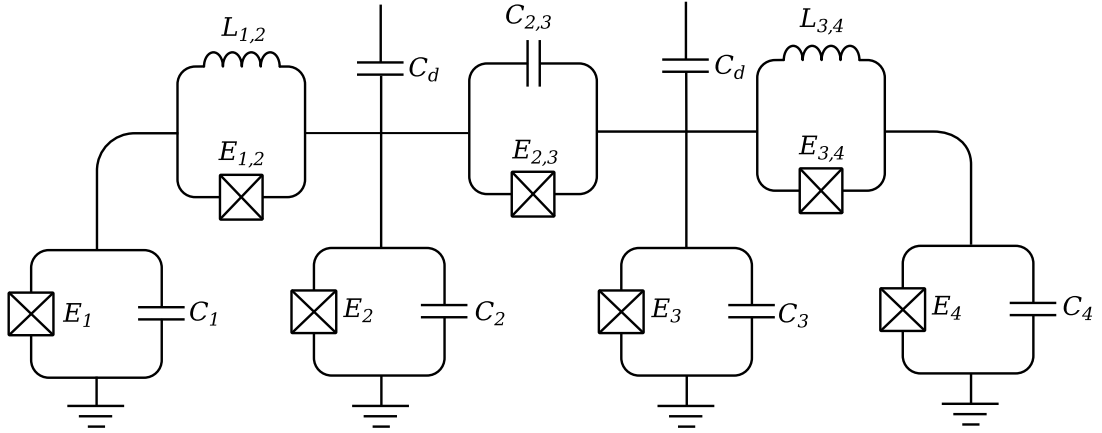


Figure 7. The lumped circuit model. Four grounded C-shunted flux qubits are connected through Josephson junctions and alternating inductors and capacitors.

N , actually it is as simple as expanding the capacitance matrix in Eq. (41). Following the procedure of Refs. [40, 53] we obtain the following Lagrangian

$$L = 2 \sum_{i=1}^N C_i \dot{\phi}_i^2 + 2 \sum_{i=1}^{N-1} C_{i,i+1} (\dot{\phi}_i - \dot{\phi}_{i+1})^2 + \sum_{i=1}^N E_i \cos \phi_i + \sum_{i=1}^{N-1} E_{i,i+1} \cos (\phi_i - \phi_{i+1}) - \frac{1}{2} \sum_{i=1}^{N-1} \frac{(2\pi)^2}{L_{i,i+1}} (\phi_i - \phi_{i+1})^2, \quad (40)$$

where the first two terms come from the capacitors and are interpreted as the kinetic terms, while the remaining terms come from the Josephson junctions and inductors and are interpreted as the potential terms. Note that in the present case $C_{1,2} = C_{3,4} = 0$ and $1/L_{2,3} = 0$. Also note that the driving capacitances from the control lines are not in the Lagrangian, since they are in parallel with the shunting capacitances, C_i they can simply be added to those. The capacitance matrix becomes

$$K = 8 \begin{pmatrix} C_1 & 0 & 0 & 0 \\ 0 & C_2 + C_{2,3} & -C_{2,3} & 0 \\ 0 & -C_{2,3} & C_3 + C_{2,3} & 0 \\ 0 & 0 & 0 & C_4 \end{pmatrix}, \quad (41)$$

which we note is a block diagonal matrix, hence its inverse matrix must be likewise, which means that the only couplings due to the capacitances are between node 2 and 3. With the capacitance matrix we can write the Hamiltonian as

$$H = 4\mathbf{p}^T K^{-1} \mathbf{p} + U(\phi), \quad (42)$$

where $U(\phi)$ is the potential due to the Josephson junctions and inductors, which we will now focus on.

a. Expansion of the potential

We now do a Taylor expansion of the cosines in the potential around zero. To the desired fourth order we obtain

$$U(\phi) = \sum_{i=1}^N \left\{ \frac{E_i}{2} \phi_i^2 - \frac{E_i}{24} \phi_i^4 \right\} + \sum_{i=1}^{N-1} E_{i,i+1} \left[\frac{1}{2} (\phi_i - \phi_{i+1})^2 - \frac{1}{24} (\phi_i - \phi_{i+1})^4 \right] + \sum_{i=1}^{N-1} \frac{(2\pi)^2}{2L_{i,i+1}} (\phi_i - \phi_{i+1})^2. \quad (43)$$

Note that since cosine is an even function, no cubic terms appear in the expansion. Expanding the parenthesis, and once again removing all irrelevant constant terms yields

$$\begin{aligned} U(\phi) = & \sum_{i=1}^N \left\{ \frac{E_i}{2} \phi_i^2 - \frac{E_i}{24} \phi_i^4 \right\} + \sum_{i=1}^{N-1} \frac{(2\pi)^2}{2L_{i,i+1}} (\phi_i^2 + \phi_{i+1}^2 - 2\phi_i\phi_{i+1}) \\ & + \sum_{i=1}^{N-1} \left[\frac{E_{i,i+1}}{2} (\phi_i^2 + \phi_{i+1}^2 - 2\phi_i\phi_{i+1}) - \frac{E_{i,i+1}}{24} (\phi_i^4 + \phi_{i+1}^4 - 4\phi_i^3\phi_{i+1} + 6\phi_i^2\phi_{i+1}^2 - 4\phi_i\phi_{i+1}^3) \right]. \end{aligned}$$

As we wish to employ the rotating wave approximation later we can now remove all terms with an odd power of the nodes fluxes, meaning that the last term of inductor sum vanishes. We are now in a position to collect terms. This yields the full Hamiltonian

$$\begin{aligned} H = & \sum_{i=1}^N \left[4E_{C,i}p_i^2 + \frac{1}{2} (E_{L,i} + E_{J,i}) \phi_i^2 - \frac{E_{J,i}}{24} \phi_i^4 \right] + 8(K^{-1})_{(2,3)}p_2p_3 \\ & + \sum_{i=1}^{N-1} \left[- \left(E_{i,i+1} + \frac{(2\pi)^2}{L_{i,i+1}} \right) \phi_i\phi_{i+1} + \frac{1}{6} E_{i,i+1} (\phi_i^3\phi_{i+1} + \phi_i\phi_{i+1}^3) - \frac{1}{4} E_{i,i+1} \phi_i^2\phi_{i+1}^2 \right], \end{aligned} \quad (44)$$

where the effective energy of the capacitances, $E_{C,i}$, are equal to the corresponding diagonal elements of the inverse of the capacitance matrix. The effective Josephson energies are

$$E_{J,i} = E_i + E_{i-1,i} + E_{i,i+1}, \quad (45)$$

where $E_{0,1} = E_{N-1,N} = 0$. Similarly the effective energies of the inductors are

$$E_{L,i} = \frac{(2\pi)^2}{L_{i-1,i}} + \frac{(2\pi)^2}{L_{i,i+1}}, \quad (46)$$

where $1/L_{0,1} = 1/L_{N-1,N} = 0$. Changing into step operators we obtain

$$\begin{aligned} H = & \sum_{i=1}^N \left[S_i b_i^\dagger b_i - E_{J,i} T_i^4 (b_i^\dagger + b_i)^4 \right] + 2(K^{-1})_{(1,2)} (T_2 T_3)^{-1} (b_2^\dagger - b_2) (b_3^\dagger - b_3) \\ & + \sum_{i=1}^{N-1} \left[- \left(E_{i,i+1} + \frac{(2\pi)^2}{L_{i,i+1}} \right) T_i T_{i+1} (b_i^\dagger + b_i) (b_{i+1}^\dagger + b_{i+1}) - \frac{1}{4} E_{i,i+1} T_i^2 T_{i+1}^2 (b_i^\dagger + b_i)^2 (b_{i+1}^\dagger + b_{i+1})^2 \right. \\ & \left. + \frac{1}{6} E_{i,i+1} \left\{ T_i^3 T_{i+1} (b_i^\dagger + b_i)^3 (b_{i+1}^\dagger + b_{i+1}) + T_i T_{i+1}^3 (b_i^\dagger + b_i) (b_{i+1}^\dagger + b_{i+1})^3 \right\} \right], \end{aligned} \quad (47)$$

where we have defined

$$T_n = \left(\frac{2E_{C,n}}{E_{J,n} + E_{L,n}} \right)^{1/4}, \quad (48a)$$

$$S_n = 4 \sqrt{\frac{1}{2} E_{C,n} (E_{L,n} + E_{J,n})}. \quad (48b)$$

b. Truncating to a spin model

We are now ready to truncate the Hamiltonian in Eq. (44) into a spin model. The Hamiltonian becomes

$$\begin{aligned}
 H = & - \sum_{i=1}^N \left[\frac{1}{2} S_i - \frac{1}{4} E_{J,i} T_i^4 \right] \sigma_i^z - 2(K^{-1})_{(2,3)} (T_i T_{i+1})^{-1} \sigma_2^y \sigma_3^y \\
 & + \sum_{i=1}^{N-1} \left[- \left(E_{i,i+1} + \frac{(2\pi)^2}{L_{i,i+1}} \right) T_i T_{i+1} \sigma_i^x \sigma_{i+1}^x + \frac{1}{6} E_{i,i+1} (T_i^3 T_{i+1} \sigma_i^x \sigma_{i+1}^x + T_i T_{i+1}^3 \sigma_i^x \sigma_{i+1}^x) \right. \\
 & \left. - \frac{1}{4} E_{i,i+1} T_i^2 T_{i+1}^2 (\sigma_i^z \sigma_{i+1}^z - 2(\sigma_i^z + \sigma_{i+1}^z)) \right], \tag{49}
 \end{aligned}$$

which can be rewritten more elegantly as

$$H = - \frac{1}{2} \sum_{i=1}^N \Omega_i \sigma_i^z + 2 J_2^y \sigma_2^y \sigma_3^y + \sum_{i=1}^{N-1} \left[2 \tilde{J}_{i,i+1}^x \sigma_i^x \sigma_{i+1}^x + J_{i,i+1}^z \sigma_i^z \sigma_{i+1}^z \right], \tag{50}$$

with the spin frequencies defined as

$$\Omega_i = S_i - \frac{1}{2} E_{J,i} T_i^4 - E_{i-1,i} T_{i-1}^2 T_i^2 - E_{i,i+1} T_i^2 T_{i+1}^2, \tag{51}$$

where $T_0 = T_N = 0$. If we truncate to the three lowest states of the anharmonic oscillator, we find that the energy difference between the first and second excited state is given as

$$\Omega'_i = \Omega - \frac{1}{2} E_{J,i} T_i^4. \tag{52}$$

Thus the absolute and relative anharmonicity becomes

$$\mathcal{A}_i = \Omega'_i - \Omega_i = -\frac{1}{2} E_{J,i} T_i^4, \quad \mathcal{A}_i^r = -\frac{1}{2} \frac{E_{J,i} T_i^4}{\Omega_i}. \tag{53}$$

The coupling constants are defined as

$$\tilde{J}_i^x = -\frac{1}{2} \left(E_{i,i+1} + \frac{(2\pi)^2}{L_{i,i+1}} \right) T_i T_{i+1} + \frac{1}{4} E_{i,i+1} (T_i^3 T_{i+1} + T_i T_{i+1}^3), \tag{54a}$$

$$J_i^y = - (K^{-1})_{(i,i+1)} (T_i T_{i+1})^{-1}, \tag{54b}$$

$$J_i^z = -\frac{1}{4} E_{i,i+1} (T_i T_{i+1})^2. \tag{54c}$$

By transforming into the interaction picture (using Eq. (12)) and defining $J_2^x \equiv \tilde{J}_2^x + J_2^y$ we arrive at the Hamiltonian in Eq. (3) after doing the rotating wave approximation.

4. State preparation driving scheme

In order to operate the gate successively, we need a scheme for preparing the state of the gate. We would like to be able to address the gate exclusively, i.e. opening and closing the gate independently of the left and right qubits. This is possible when the outer qubits are detuned from the gate qubits, i.e. Δ is sufficiently large, compared to the couplings between the gate qubits and the outer qubits. A large detuning can, in experiments, be obtained by tuning the external fluxes.

We can achieve control of the gate by driving node 2 and 3. This is done by adding capacitors with capacitance C_d to the design of the circuit, connecting the nodes ϕ_2 and ϕ_3 to an external field φ_d respectively.

The addition of these additional capacitors generates the following extra term in the Lagrangian

$$L_d = \frac{C_d}{2} (\dot{\phi}_2 - \dot{\varphi}_d)^2 + \frac{C_d}{2} (\dot{\phi}_3 - \dot{\varphi}_d)^2. \tag{55}$$

We now assume that the external field is given as

$$\varphi_d = \tilde{A}s(t) \sin(\omega t + \theta), \quad \dot{\varphi}_d = \tilde{A}\omega \cos(\omega t + \theta), \quad (56)$$

where $s(t)$ is some envelope function, \tilde{A} is the amplitude of the driving, ω is the driving frequency, and θ is the phase. We rewrite the driving function as

$$\begin{aligned} \varphi_d &= \tilde{A}s(t) \sin(\omega t + \theta) \\ &= \tilde{A}s(t) (\cos \theta \sin \omega t + \sin \theta \cos \omega t) \\ &= \tilde{A}(I(t) \sin \omega t + Q(t) \cos \omega t), \end{aligned}$$

where we have adopted the definitions $I(t) = s(t) \cos \theta$ for the in-phase component and $Q(t) = s(t) \sin \theta$ for the out-of-phase component.

Expanding the parenthesis yields

$$L_d = \frac{C_d}{2} \left[\dot{\phi}_2^2 + \dot{\phi}_3^2 + 2(\tilde{A}\omega \cos(\omega t + \theta))^2 - 2\tilde{A}\omega \cos(\omega t + \theta)(\dot{\phi}_2 + \dot{\phi}_3) \right]. \quad (57)$$

The first two terms are kinetic terms which can be added to the diagonal of the capacitance matrix, the third term is some irrelevant offset term, while the last term can be used to drive the system. The conjugated momentum is altered slightly

$$\mathbf{p} = K\dot{\phi} + \mathbf{d}, \quad (58)$$

where $\mathbf{d}^T = 2\tilde{A}\omega \cos \omega t (0, 1, 1, 0)$, and thus

$$\dot{\phi} = K^{-1}(\mathbf{p} - \mathbf{d}). \quad (59)$$

This changes the kinetic part of the Hamiltonian into

$$\begin{aligned} H_{\text{kin}} &= 4(\mathbf{p} - \mathbf{d})^T K^{-1}(\mathbf{p} - \mathbf{d}) \\ &= 4\mathbf{p}^T K^{-1}\mathbf{p} + 4\mathbf{d}^T K^{-1}\mathbf{d} - 4\mathbf{p}^T K^{-1}\mathbf{d} - 4\mathbf{d}^T K^{-1}\mathbf{p}, \end{aligned}$$

where the first term is the original kinetic term, the second term is some irrelevant offset while the last two terms are identical driving terms yielding

$$H_d = -8\dot{\varphi} \{ [(K^{-1})_{(2,2)} + (K^{-1})_{(3,2)}] p_2 + [(K^{-1})_{(2,3)} + (K^{-1})_{(3,3)}] p_3 \}, \quad (60)$$

which can easily be truncated to a spin model

$$H_d = \frac{1}{2} A (I(t) \sin \omega t + Q(t) \cos \omega t) (\sigma_2^y + \sigma_3^y), \quad (61)$$

where

$$A = -8\tilde{A}\omega ((K^{-1})_{(2,2)} + (K^{-1})_{(3,2)}) T_2^{-1}. \quad (62)$$

With this we are now ready to change to the interaction picture using the non-interacting Hamiltonian of Eq. (12)

$$\begin{aligned} (H_d)_I &= \frac{i}{2} A (I(t) \sin \omega t + Q(t) \cos \omega t) [(\sigma_2^- + \sigma_3^-) e^{i\Omega_1 t} - (\sigma_2^+ + \sigma_3^+) e^{-i\Omega_1 t}] \\ &= A (I(t) \sin \omega t + Q(t) \cos \omega t) [(\sigma_2^y + \sigma_3^y) \cos \Omega_1 t - (\sigma_2^x + \sigma_3^x) \sin \Omega_1 t] \\ &= \frac{A}{2} [I(t) (\sin \delta t (\sigma_2^y + \sigma_3^y) - \cos \delta t (\sigma_2^x + \sigma_3^x)) + Q(t) (\cos \delta t (\sigma_2^y + \sigma_3^y) - \sin \delta t (\sigma_2^x + \sigma_3^x))], \end{aligned}$$

where we have introduced the parameter $\delta = \omega - \Omega_1$ and we have thrown away all fast rotating terms i.e. terms with $\omega + \Omega_1$. The out-of-phase part of the driving Hamiltonian can be used to minimize leakage to the higher excited states during the driving when the anharmonicity is small [55, 56], using the CRAB driving scheme [57, 58] or the GRAPE driving scheme [59–61].

Like the rest of the Hamiltonian this term preserves the total spin of the two gate qubits, hence it does not mix the singlet and triplet states (note that the spin projection is not preserved, which is why the gate can be driven between

the different states). We can therefore ignore the singlet state $|1^-\rangle_C$, when starting from any of the triplet states shown in Fig. 3. The energies difference between the triplet states is found by

$$\langle 11| H |11\rangle_C = \Omega_2 + J_2^z, \quad (63a)$$

$$\frac{1}{2} (\langle 10| + \langle 01|) H (|10\rangle_C + |01\rangle_C) = -J_2^z + 2J_2^x, \quad (63b)$$

$$\langle 00| H |00\rangle_C = -\Omega_2 + J_2^z, \quad (63c)$$

Rabi oscillations between the closed and open states are then generated by the driving provided the driving frequency matches the energy difference $\omega = |\Omega - 2J_2^z + 2J_2^x|$ and $A \ll J_2^z$. A π -pulse, $At = \pi$, would then shift between the $|0\rangle_C$ and $|1^+\rangle$ states in a few microseconds depending on the size of A . Thus using this scheme we can drive between an open and closed gate using merely an external microwave drive.

5. Including the second excited states of the gate

In order to fulfill the requirement of $J_2 \gg J_1$ and still keep a short gate time the coupling between the control qubits, J_2 , must be rather large. This yields the concern of leakage to higher excited states. We therefore need to consider when this becomes a problem. To do this we change the control qubits in to qutrits and investigate the chain in this case. Starting from Eq. (47) we wish to truncate the middle two qubits into qutrits.

Due to the rather large expression it is advantageous to express part of the Hamiltonian at a time. Starting with the non-interacting part of the qutrit Hamiltonian in Eq. (47), i.e. the terms $i = 2, 3$ in the first sum, we obtain

$$H_{0,i} \sim \begin{pmatrix} 0 & 0 & -\sqrt{2}E_{J,i}T_i^4/4 \\ 0 & S_i - E_{J,i}T_i^4/2 & 0 \\ -\sqrt{2}E_{J,i}T_i^4/4 & 0 & 2S_i - 3E_{J,i}T_i^4/2 \end{pmatrix}, \quad (64)$$

where we have subtracted some irrelevant offset term. Note that the T coefficients are the same for both $i = 2$ and 3 due to the symmetry of the circuit. From the matrix representation, we see that there is a coupling between the ground and second excited state. This coupling is unwanted and will, like every other odd powers of couplings, disappear during the rotating wave approximation. For convenience we write the Hamiltonian using braket notation, since spin matrices does not turn out to be a good desirable basis in our case

$$H_{0,i} = \left(S_i - \frac{1}{2}E_{J,i}T_i^4 \right) |1\rangle\langle 1| + \left(2S_i - \frac{3}{2}E_{J,i}T_i^4 \right) |2\rangle\langle 2| - \frac{\sqrt{2}}{4}E_{J,i}T_i^4 (|0\rangle\langle 2| + |2\rangle\langle 0|). \quad (65)$$

We skip the rest of the non-interacting Hamiltonian for now, since it turns out that there are contributions to the energies of the states from the interacting part of the Hamiltonian.

For convenience we start by expressing the step-operators in the three level model in braket notation

$$b_i^\dagger \pm b_i = |1\rangle\langle 0|_i \pm |0\rangle\langle 1|_i + \sqrt{2}(|2\rangle\langle 1|_i \pm |1\rangle\langle 2|_i), \quad (66a)$$

$$(\hat{b}_i^\dagger + \hat{b}_i)^2 = |0\rangle\langle 0|_i + 3|1\rangle\langle 1|_i + 5|2\rangle\langle 2|_i + \sqrt{2}(|2\rangle\langle 0|_i \pm |0\rangle\langle 2|_i), \quad (66b)$$

$$(\hat{b}_i^\dagger + \hat{b}_i)^3 = |1\rangle\langle 0|_i + |0\rangle\langle 1|_i + \sqrt{2}(|2\rangle\langle 0|_i + |0\rangle\langle 2|_i). \quad (66c)$$

Thus we are ready to consider the target and control qubit x -interaction with

$$H_{T,C}^x = K_{T,C}^x \sigma_T^x \left[|1\rangle\langle 0|_C + |0\rangle\langle 1|_C + \sqrt{2}(|2\rangle\langle 1|_C + |1\rangle\langle 2|_C) \right] + M_{T,C}^x \sigma_T^x \left[|1\rangle\langle 0|_C + |0\rangle\langle 1|_C + 2\sqrt{2}(|2\rangle\langle 1|_C + |1\rangle\langle 2|_C) \right], \quad (67)$$

where we use the notation that as a subscript we have either $T = 1, 4$ and $C = 2, 3$ in pairs. We have defined

$$K_{i,j}^x = - \left(E_{i,j} + \frac{(2\pi)^2}{L_{i,j}} \right) T_i T_j + \frac{1}{6} E_{i,j} T_i^3 T_j, \quad (68a)$$

$$M_{i,j}^x = \frac{1}{6} E_{i,j} T_i T_j^3. \quad (68b)$$

Note that $2\tilde{J}_1^x = K_{T,C}^x + M_{T,C}^x$, however, due to the factor of 2 on the last term in $\hat{H}_{T,C}^x$, we cannot use \tilde{J}_1^x . The next term we consider is the z -interaction between the target and control qubit

$$H'_{T,C} = J_1^z(2\mathbb{1} - \sigma_T^z) \left[|0\rangle\langle 0|_C + 3|1\rangle\langle 1|_C + 5|2\rangle\langle 2|_C + \sqrt{2}(|2\rangle\langle 0|_C + |0\rangle\langle 2|_C) \right], \quad (69)$$

where J_1^z can be found in Eq. (54c). From this we realize that we obtain not only z -interactions, but also corrections to the energies of the qutrits and some terms involving $|2\rangle\langle 0|$, which will disappear during the rotating wave approximation, if the conditions are right. Therefore we define

$$H_{T,C}^z = J_1^z\sigma_T^z \left[|0\rangle\langle 0|_C - |1\rangle\langle 1|_C - 3|2\rangle\langle 2|_C - \sqrt{2}(|2\rangle\langle 0|_C + |0\rangle\langle 2|_C) \right], \quad (70)$$

while we add the contribution to the qutrit energy to the non-interacting Hamiltonian.

This leaves only the interaction between the two control qutrits. We start with their y -interaction

$$H_{2,3}^y = -2J_2^y \prod_{i=2}^3 \left[|1\rangle\langle 0|_i - |0\rangle\langle 1|_i + \sqrt{2}(|2\rangle\langle 1|_i - |1\rangle\langle 2|_i) \right], \quad (71)$$

where J_2^y is defined in Eq. (54b). Moving on to the x -interaction

$$\begin{aligned} H_{2,3}^x = & K_{2,3}^x \prod_{i=2}^3 \left[(|1\rangle\langle 0|_i + |0\rangle\langle 1|_i) + \sqrt{2}(|2\rangle\langle 1|_i + |1\rangle\langle 2|_i) \right] \\ & + M_{2,3}^x \prod_{i=2}^3 \left[(|1\rangle\langle 0|_i + |0\rangle\langle 1|_i) + 2\sqrt{2}(|2\rangle\langle 1|_i + |1\rangle\langle 2|_i) \right]. \end{aligned} \quad (72)$$

This leaves the z -interaction

$$\begin{aligned} H'_{2,3} = & J_2^z \prod_{i=2}^3 \left[|0\rangle\langle 0|_i + 3|1\rangle\langle 1|_i + 5|2\rangle\langle 2|_i + \sqrt{2}(|2\rangle\langle 0|_i + |0\rangle\langle 2|_i) \right] \\ = & J_2^z \prod_{i=2}^3 \left[2\mathbb{1} - |0\rangle\langle 0|_i + |1\rangle\langle 1|_i + 3|2\rangle\langle 2|_i + \sqrt{2}(|2\rangle\langle 0|_i + |0\rangle\langle 2|_i) \right] \\ = & -2J_2^z \sum_{i=2}^3 \left[|0\rangle\langle 0|_i - |1\rangle\langle 1|_i - 3|2\rangle\langle 2|_i - \sqrt{2}(|2\rangle\langle 0|_i + |0\rangle\langle 2|_i) \right] \\ & + J_2^z \prod_{i=2}^3 \left[|0\rangle\langle 0|_i - |1\rangle\langle 1|_i - 3|2\rangle\langle 2|_i - \sqrt{2}(|2\rangle\langle 0|_i + |0\rangle\langle 2|_i) \right], \end{aligned} \quad (73)$$

where we have thrown away some irrelevant offset term. Once again we find a contribution to the qutrit energy, and some terms related to $|2\rangle\langle 0|$, and therefore we only consider the last product as the z -interaction calling it $H_{2,3}^z$. This was the last part of the Hamiltonian and thus the last addition to the energy of the qutrits. Now we can write the full non-interacting Hamiltonian as

$$H_0 = -\frac{1}{2}\Omega_1(\sigma_1^z + \sigma_4^z) - \frac{1}{2}\Omega_2(|0\rangle\langle 0|_2 - |1\rangle\langle 1|_2 + |0\rangle\langle 0|_3 - |1\rangle\langle 1|_3) + \frac{1}{2}(\Omega_2 + 2\Omega'_2)(|2\rangle\langle 2|_2 + |2\rangle\langle 2|_3), \quad (74)$$

where Ω_i can be found in Eq. (51). Lastly the energy up to the new state is given in Eq. (52) and thus in general we would expect $\Omega_2 \neq \Omega'_2$ due to the anharmonicity which can be found in Panel B of ???. A schematic drawing of the system consisting of an input qubit, two gate qutrits, and an output qubit can be seen in Fig. 8.

Collecting all terms the full Hamiltonian becomes

$$H = H_0 + \sum_{i=1}^3 (\hat{H}_{i,i+1}^x + \hat{H}_{i,i+1}^z) + \hat{H}_{2,3}^y + 2\sqrt{2}(J_1^z + J_2^z)(|2\rangle\langle 0|_2 + |0\rangle\langle 2|_2 + |2\rangle\langle 0|_3 + |0\rangle\langle 2|_3). \quad (75)$$

We now choose our non-interacting Hamiltonian completely equivalent to previously, but with the addition of the second excited state

$$H_0 = -\frac{1}{2}\Omega_1(\sigma_1^z + \sigma_4^z) - \frac{1}{2}\Omega_1(|0\rangle\langle 0|_2 - |1\rangle\langle 1|_2 + |0\rangle\langle 0|_3 - |1\rangle\langle 1|_3) + \frac{1}{2}(\Omega_2 + 2\Omega'_2)(|2\rangle\langle 2|_2 + |2\rangle\langle 2|_3), \quad (76)$$

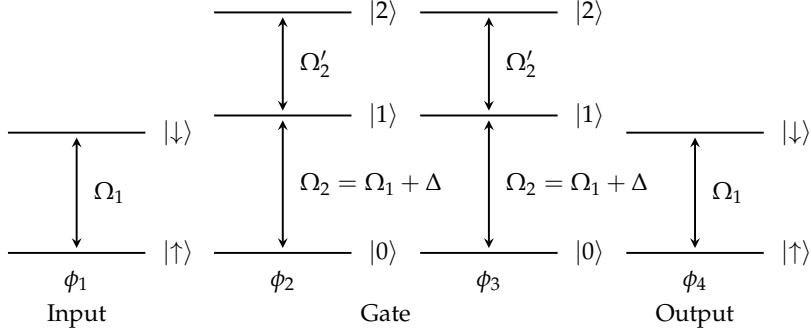


Figure 8. Sketch of the quantum spin gate chain where the third states of the controls have been included, changing the gate into consisting of two qubits. The energy distance between each state has been included in the drawing. The system is the same for the pure qubit gate, just with the two highest levels removed.

and we wish to perform the rotating wave approximation. All odd powers of exchange operators disappear, as long as the energy between the two states are large enough. In our case this is always the case and thus the last term of Eq. (75) disappears. Consider now the x -interaction parts $\hat{H}_{T,C}^x$. We write the Pauli x -operator as $\sigma_T^x = |1\rangle\langle 0|_T + |0\rangle\langle 1|_T$ in order to make the notation more obvious. When combined with the qutrits. Thus it becomes obvious that permutations of $|1\rangle\langle 0|_T |0\rangle\langle 1|_C$ will survive. This is exactly equivalent with the surviving cases of the qubits. Similarly permutations of $|1\rangle\langle 0|_T |1\rangle\langle 2|_C$ can only survive if $\Omega'_2 \sim \Omega_1$. This leaves

$$(H_{T,C}^x)_I = J_1^x (|0\rangle\langle 1|_T |1\rangle\langle 0|_C + |1\rangle\langle 0|_T |0\rangle\langle 1|_C) + \sqrt{2}(K_{T,C}^x + 2M_{T,C}^x) (|0\rangle\langle 1|_T |2\rangle\langle 1|_C e^{i(\Omega_1 - \Omega'_2)t} + |1\rangle\langle 0|_T |1\rangle\langle 2|_C e^{-i(\Omega_1 - \Omega'_2)t}). \quad (77)$$

However, if $|\Omega_1 - \Omega'_2| \gg |\sqrt{2}(K_{T,C}^x + 2M_{T,C}^x)|$ the last two terms will rotate away as well. As $|\sqrt{2}(K_{T,C}^x + 2M_{T,C}^x)|$ is usually the close to the size of the coupling J_1^x when we configure the circuit as a the swapping gate these term will almost always rotate away. We are left with

$$(H_{T,C}^x)_I = J_1^x (|0\rangle\langle 1|_T |1\rangle\langle 0|_C + |1\rangle\langle 0|_T |0\rangle\langle 1|_C), \quad (78)$$

and the interaction resembles the original interaction for when the chain was entirely qubits.

Turning to $\hat{H}_{T,C}^z$ we see that only the last two terms containing $|2\rangle\langle 0|_C$ and $|0\rangle\langle 2|_C$ obtain a phase factor of $e^{i(E_1 + E_2)t}$, which makes the terms rotate away, and thus the Hamiltonian becomes

$$(H_{T,C}^z)_I = J_1^z \sigma_T^z (|0\rangle\langle 0|_C - |1\rangle\langle 1|_C - 3|2\rangle\langle 2|_C). \quad (79)$$

The last part of the Hamiltonian is the interaction between the gate qutrits. Starting from the x - and y -interaction, which we can deal with together since only a sign differs, we realize that the terms $|0\rangle\langle 1|_i$ receives a phase of $e^{i\Omega_2 t}$, while terms on the form $|1\rangle\langle 2|_i$ receive a phase of $e^{i\Omega'_2 t}$. Thus taking the products in Eqs. (71) and (72) we realize that all phases with a sum of Ω'_2 and/or Ω_2 rotate away rapidly, while terms with differences are kept. Thus focusing on Eq. (71) we obtain

$$(H_{2,3}^y)_I = 2J_2^y \left[|1\rangle\langle 0|_2 |0\rangle\langle 1|_3 + |1\rangle\langle 0|_2 |0\rangle\langle 1|_3 + 2(|2\rangle\langle 1|_2 |1\rangle\langle 2|_3 + |1\rangle\langle 2|_2 |2\rangle\langle 1|_3) + \sqrt{2} \left(\{|2\rangle\langle 1|_2 |0\rangle\langle 1|_3 + |0\rangle\langle 1|_2 |2\rangle\langle 1|_3\} e^{i(\Omega_2 - \Omega'_2)t} + \{|1\rangle\langle 2|_2 |1\rangle\langle 0|_3 + |1\rangle\langle 0|_2 |1\rangle\langle 2|_3\} e^{-i(\Omega_2 - \Omega'_2)t} \right) \right]. \quad (80)$$

The products in Eq. (72) are handled identically yielding a total x - and y -interaction term

$$(H_{2,3}^{xy})_I = 2J_2^x (|1\rangle\langle 0|_2 |0\rangle\langle 1|_3 + |1\rangle\langle 0|_2 |0\rangle\langle 1|_3) + 4R_{2,3}^x (|2\rangle\langle 1|_2 |1\rangle\langle 2|_3 + |1\rangle\langle 2|_2 |2\rangle\langle 1|_3) + 2\sqrt{2}P_{2,3}^x \left(\{|2\rangle\langle 1|_2 |0\rangle\langle 1|_3 + |0\rangle\langle 1|_2 |2\rangle\langle 1|_3\} e^{i(\Omega_2 - \Omega'_2)t} + \{|1\rangle\langle 2|_2 |1\rangle\langle 0|_3 + |1\rangle\langle 0|_2 |1\rangle\langle 2|_3\} e^{-i(\Omega_2 - \Omega'_2)t} \right), \quad (81)$$

where we have set $R_{2,3}^x = J_2^y + K_{2,3}^x + 4M_{2,3}^x$ and $P_{2,3}^x = J_2^y + K_{2,3}^x + 2M_{2,3}^x$. Thus if the anharmonicity is large enough such that $|\Omega_2 - \Omega'_2| \gg 2\sqrt{2}|J_2^y + K_{2,3}^x + 2M_{2,3}^x|$ the last four terms will rotate away and the third level will

be completely decoupled from the two lowest states. However, in our case we require the coupling between the two control qubits/qutrits to be strong and thus the anharmonicity will not be large enough to rotate these terms away. However, we do not expect this to be a problem since the swapping is only inside the gate, and a closed gate never consists of enough excitation to reach any state higher than the first excited state.

Lastly we have the z -interaction between the gate qutrits. This is handled equivalently to Eq. (79) and after the fast rotating terms have been removed we obtain

$$(H_{2,3}^z)_I = J_2^z (|0\rangle\langle 0|_2 - |1\rangle\langle 1|_2 - 3|2\rangle\langle 2|_2) (|0\rangle\langle 0|_3 - |1\rangle\langle 1|_3 - 3|2\rangle\langle 2|_3) + 2J_2^z (|2\rangle\langle 0|_2 |0\rangle\langle 2|_3 + |0\rangle\langle 2|_2 |2\rangle\langle 0|_3), \quad (82)$$

where the second term is a swap-term between a double excitation of the two qutrits, and will probably not make much difference since our trouble starts when any of the two qutrits become double excited, and thus a swap of the doubly excited qutrits is irrelevant for us.

Combining the above parts of the full Hamiltonian in the interaction picture we obtain

$$\begin{aligned} H = & -\frac{1}{2}\Delta (|0\rangle\langle 0|_2 - |1\rangle\langle 1|_2 + |0\rangle\langle 0|_3 - |1\rangle\langle 1|_3) + 2J_1^x (|0\rangle\langle 1|_1 |1\rangle\langle 0|_2 + |1\rangle\langle 0|_1 |0\rangle\langle 1|_2) \\ & + J_1^z (|0\rangle\langle 0|_1 - |1\rangle\langle 1|_1) (|0\rangle\langle 0|_2 - |1\rangle\langle 1|_2 - 3|2\rangle\langle 2|_2) \\ & + J_2^z (|0\rangle\langle 0|_2 - |1\rangle\langle 1|_2 - 3|2\rangle\langle 2|_2) (|0\rangle\langle 0|_3 - |1\rangle\langle 1|_3 - 3|2\rangle\langle 2|_3) \\ & + 2J_2^z (|2\rangle\langle 0|_2 |0\rangle\langle 2|_3 + |0\rangle\langle 2|_2 |2\rangle\langle 0|_3) + 2J_2^x (|0\rangle\langle 1|_2 |1\rangle\langle 0|_3 + |1\rangle\langle 0|_2 |0\rangle\langle 1|_3) \\ & + 4R_{2,3}^x (|2\rangle\langle 1|_2 |1\rangle\langle 2|_3 + |1\rangle\langle 2|_2 |2\rangle\langle 1|_3) \\ & + 2\sqrt{2}P_{2,3}^x \left(\{|2\rangle\langle 1|_2 |0\rangle\langle 1|_3 + |0\rangle\langle 1|_2 |2\rangle\langle 1|_3\} e^{i(\Omega_2 - \Omega'_2)t} + \{|1\rangle\langle 2|_2 |1\rangle\langle 0|_3 + |1\rangle\langle 0|_2 |1\rangle\langle 2|_3\} e^{-i(\Omega_2 - \Omega'_2)t} \right) \\ & + 2J_{3,4}^x (|0\rangle\langle 1|_4 |1\rangle\langle 0|_3 + |1\rangle\langle 0|_4 |0\rangle\langle 1|_3) + J_{3,4}^z (|0\rangle\langle 0|_4 - |1\rangle\langle 1|_4) (|0\rangle\langle 0|_3 - |1\rangle\langle 1|_3 - 3|2\rangle\langle 2|_3). \end{aligned} \quad (83)$$

While this Hamiltonian looks rather everlasting, we realize that it is still excitation preserving, and we can thus consider each subspace, \mathcal{B}_k , where $k = 0, \dots, 6$, individually. By comparing the new three state Hamiltonian in Eq. (83), with the old spin Hamiltonian in Eq. (3), we see that the system behaves identically within these subspaces.

The only remaining subspaces we need to consider is \mathcal{B}_2 and \mathcal{B}_3 . The subspace \mathcal{B}_2 in Appendix 3 with the addition of the two states $|0200\rangle$ and $|0020\rangle$. Thus we only need to calculate the part of the Hamiltonian concerning these two states, as the rest is calculated in Eq. (12). This gives us the block matrix

$$H_2 = \left(\begin{array}{c|c} H_0 & W^\dagger \\ \hline W & V \end{array} \right), \quad (84)$$

where

$$V = \begin{pmatrix} \Delta/2 - 3J_2^z - 3J_1^z & 2J_2^z \\ 2J_2^z & \Delta/2 - 3J_2^z - 3J_1^z \end{pmatrix}, \quad (85a)$$

$$W = 2\sqrt{2}P_{2,3}^x e^{i(\Omega_2 - \Omega'_2)t} \begin{pmatrix} 0 & 0 & 1 & 0 & 0 & 0 \\ 0 & 0 & 1 & 0 & 0 & 0 \end{pmatrix}, \quad (85b)$$

and H_0 is given in Eq. (11). From this we see that the addition of the two new states only interfere with the state $|0110\rangle$, thus we can perform our coordinate transformation of Eq. (17) to H_0 as before, without affecting any of the new states. The conclusion to this is that the states $|0\psi_{\pm}1\rangle$ and $|1\psi_{\pm}0\rangle$ are still approximate eigenstates and thus stationary, however, $|0110\rangle$ is no longer an eigenstate. Thus we still have a closed gate, as long as the remaining three eigenstates are not in resonance with the closed state. We do not calculate these eigenstates here, but it is sufficient to say that they are not in resonance.

Due to inclusion of the third states the resonance between the states $|1001\rangle$ and $|1\psi_{\mp}0\rangle$ and $|0\psi_{\mp}1\rangle$ only hold approximately meaning that the oscillation between these three states is slowed down.

6. Full capacitive couplings

In this appendix we consider the case where all qubits are coupled entirely with capacitors. This is equivalent to the model proposed in Ref. [48].

Consider the circuit in Fig. 9, which is N qubits in series with inductors of alternating size. This circuit yields a Lagrangian of

$$L = \sum_{n=1}^N \left(\frac{1}{2}C_i \dot{\phi}_i^2 + E_i \cos \phi_i \right), \quad (86)$$

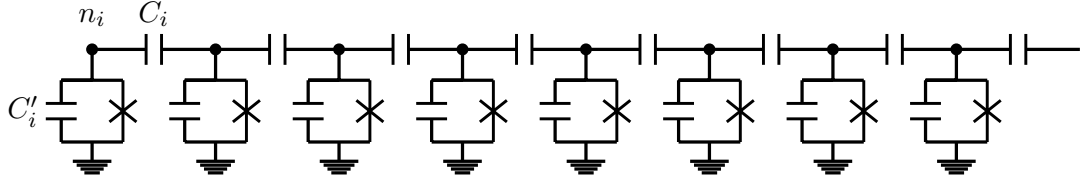


Figure 9. The circuit consists of N qubits connected through capacitors of size C_i . Each Transmon consist of a capacitor of size C'_i and a Josephson junction (usually a SQUID) of size E_i . The nodes of the circuit is denoted n_i .

This yields a Hamiltonian of

$$H = 4\mathbf{p}^T K^{-1} \mathbf{p} - \sum_{n=1}^N E_i \cos \phi_i. \quad (87)$$

Now consider that we want identical couplings between all of the qubits we therefore set $C_i = C'_i = C$ which yields the following inverse capacitance matrix here for the simple case of $N = 4$

$$K^{-1} = \frac{1}{C} \begin{pmatrix} 1 & 0 & -1 & 1 \\ 0 & 0 & 1 & -1 \\ -1 & 1 & 0 & 0 \\ 1 & -1 & 0 & 1 \end{pmatrix}. \quad (88)$$

From this we see that the desired nearest neighbor coupling simply disappear between some of the qubits, while couplings beyond nearest neighbor is significant. Increasing the number of qubits does not fix this. In fact in all cases where $N + 1$ is dividable with 3 the matrix is even singular. One could try to fix this simply by increasing size of the shunting capacitor C'_i of the qubit compared to the coupling capacitor C_i . Thus for $C'_i = 10C_i = 10C$ we get

$$K^{-1} \simeq \frac{1}{C} \begin{pmatrix} 0.1 & 0.01 & 0.001 & 0.0001 \\ 0.01 & 0.1 & 0.01 & 0.001 \\ 0.001 & 0.01 & 0.1 & 0.01 \\ 0.0001 & 0.001 & 0.01 & 0.1 \end{pmatrix}, \quad (89)$$

which does indeed seem to fix the problem. Consider now the case where we want to make a SSH chain such as in Ref [48]. In this case, we alternate the coupling between the qubits such that in the case of $N = 6$

$$K^{-1} = \begin{pmatrix} C'_1 & C & 0 & 0 & 0 & 0 \\ C & C'_2 & 2C & 0 & 0 & 0 \\ 0 & 2C & C'_3 & C & 0 & 0 \\ 0 & 0 & C & C'_4 & 2C & 0 \\ 0 & 0 & 0 & 2C & C'_5 & C \\ 0 & 0 & 0 & 0 & C & C'_6 \end{pmatrix}. \quad (90)$$

For $C'_i = C$, we obtain a result similar to the one in the first example where some of the nearest neighbor couplings disappear, and couplings beyond this become large. This can be fixed using the approach as mentioned above with $C \ll C'_i$. The proposal of Ref. [48] suggests to take $C \gg C'_i$ in order to enter the strong-coupling regime and realize a linear SSH chain. Given the above analysis, we cannot see how this is feasible without some other modifications to the circuit.

The superconducting qubit should instead be connected with inductors or connected with alternating inductors and capacitors in order to avoid cross talk. However, it is still not enough to alternate between the sizes of the inductors or capacitors if the chain is of finite length, due to end point irregularities.